



# Ice core records of climate variability on the Third Pole with emphasis on the Guliya ice cap, western Kunlun Mountains

Lonnie G. Thompson<sup>a, b, \*</sup>, Tandong Yao<sup>c</sup>, Mary E. Davis<sup>a</sup>, Ellen Mosley-Thompson<sup>a, d</sup>, Guangjian Wu<sup>c</sup>, Stacy E. Porter<sup>a</sup>, Baiqing Xu<sup>c</sup>, Ping-Nan Lin<sup>a</sup>, Ninglian Wang<sup>e</sup>, Emilie Beaudon<sup>a</sup>, Keqin Duan<sup>f</sup>, M. Roxana Sierra-Hernández<sup>a</sup>, Donald V. Kenny<sup>a</sup>

<sup>a</sup> Byrd Polar and Climate Research Center, The Ohio State University, Columbus, OH, 43210, USA

<sup>b</sup> School of Earth Sciences, The Ohio State University, Columbus, OH, 43210, USA

<sup>c</sup> Key Laboratory of Tibetan Climate Changes and Land Surface Processes, Institute of Tibetan Plateau Research, Chinese Academy of Sciences, Beijing, China

<sup>d</sup> Department of Geography, The Ohio State University, Columbus, OH, 43210, USA

<sup>e</sup> College of Urban and Environmental Science, Northwest University, Xian, China

<sup>f</sup> College of Tourism and Environmental Science, Shaanxi Normal University, Xian, China

## ARTICLE INFO

### Article history:

Received 30 October 2017

Received in revised form

5 February 2018

Accepted 5 March 2018

### Keywords:

Ice cores

Present

Paleoclimatology

China

Monsoon

Stable isotopes

North Atlantic

Glaciology

## ABSTRACT

Records of recent climate from ice cores drilled in 2015 on the Guliya ice cap in the western Kunlun Mountains of the Tibetan Plateau, which with the Himalaya comprises the Third Pole (TP), demonstrate that this region has become warmer and moister since at least the middle of the 19th century. Decadal-scale linkages are suggested between ice core temperature and snowfall proxies, North Atlantic oceanic and atmospheric processes, Arctic temperatures, and Indian summer monsoon intensity. Correlations between annual-scale oxygen isotopic ratios ( $\delta^{18}\text{O}$ ) and tropical western Pacific and Indian Ocean sea surface temperatures are also demonstrated. Comparisons of climate records during the last millennium from ice cores acquired throughout the TP illustrate centennial-scale differences between monsoon and westerlies dominated regions. Among these records, Guliya shows the highest rate of warming since the end of the Little Ice Age, but  $\delta^{18}\text{O}$  data over the last millennium from TP ice cores support findings that elevation-dependent warming is most pronounced in the Himalaya. This, along with the decreasing precipitation rates in the Himalaya region, is having detrimental effects on the cryosphere. Although satellite monitoring of glaciers on the TP indicates changes in surface area, only a few have been directly monitored for mass balance and ablation from the surface. This type of ground-based study is essential to obtain a better understanding of the rate of ice shrinkage on the TP.

© 2018 Elsevier Ltd. All rights reserved.

## 1. Introduction

The Third Pole (TP), which is composed of the Tibetan Plateau and the Himalaya, is the core of High Asia, a region that contains an ice cover of over 100,000 km<sup>2</sup> (Dyurgerov et al., 2002; Yao et al., 2012). Within western China, ~46,000 glaciers have a total area of ~59,000 km<sup>2</sup> (Ding et al., 2006), which constitutes one of Earth's largest stores of ice. The TP, especially the Himalaya, is also referred to as "Asia's water tower" (Immerzeel et al., 2010) as its cryosphere is a major contributor to the continent's rivers which sustain ~1.5

billion people in 10 countries. Because it is the highest and largest (5 million km<sup>2</sup>) of Earth's elevated regions, the TP has a significant role in regional and global environmental change and in Earth's climate system.

The climate of the TP is influenced by several air masses and moisture sources (Fig. 1A), including the Southeast Asian monsoon and the Southwest or Indian summer monsoon (ISM) systems and the continental westerlies (Tian et al., 2001, 2003; Yao et al., 2013). The mountain systems along the southern periphery are impacted primarily by the summer monsoons and the northwestern and northern regions are influenced by the westerlies throughout the year (Tian et al., 2007). However, some of the precipitation in the arid interior is derived from continental moisture recycled from the monsoons (Dong et al., 2016; Yao et al., 2013). This tends to complicate the interpretation of precipitation chemistry such as

\* Corresponding author. Byrd Polar and Climate Research Center, The Ohio State University, 1090 Carmack Road, Columbus, OH 43210, USA.

E-mail address: [thompson.3@osu.edu](mailto:thompson.3@osu.edu) (L.G. Thompson).

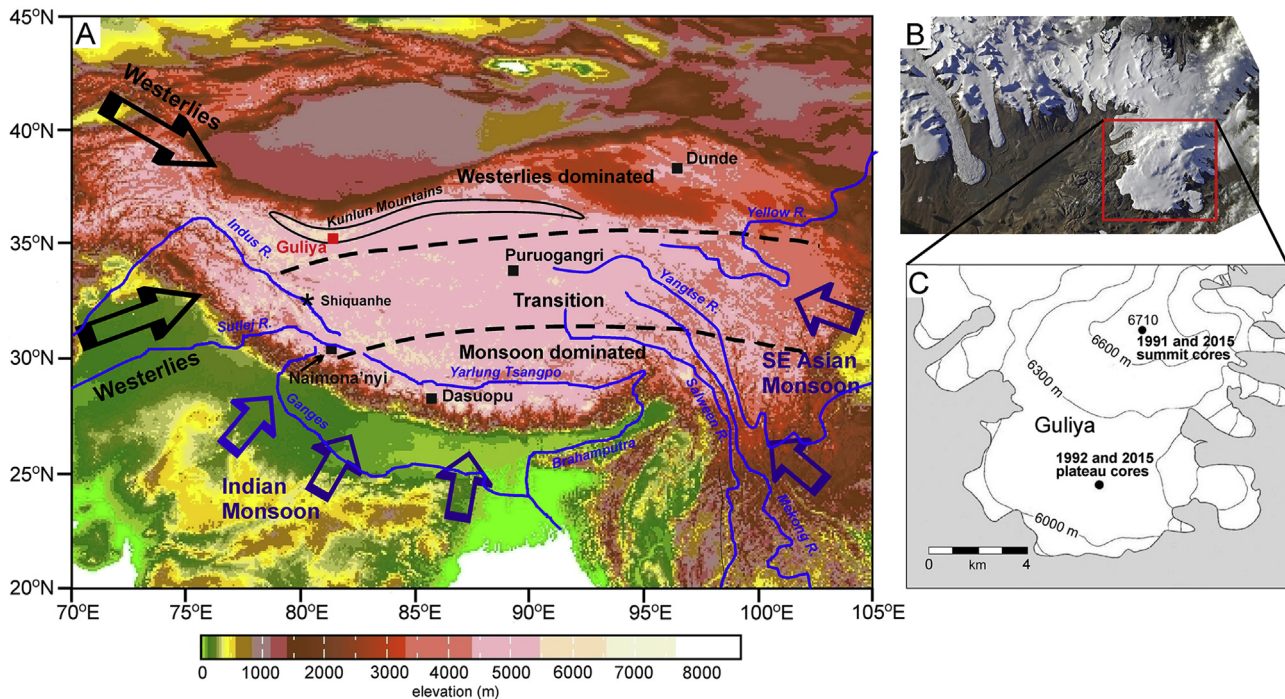


**Fig. 1.** Regional setting of Third Pole and Guliya ice cap. (A) Third Pole region and northern India showing major river systems, locations of ice core sites marked with black squares (the Guliya site is identified with a red square) and dominant air masses. The three major climate regimes (monsoon dominated in the south, westerlies dominated in the north, and the transition between westerlies and monsoon dominated) are based on Yao et al. (2013). (B) Satellite photos show the ice sheet in the western Kunlun Mountains with Guliya bordered by the red box. (C) Topographic map of the Guliya ice cap shows locations of drill sites in the early 1990s and in 2015. Relief map source: NOAA NGDC GLOBE (<http://iridl.ldeo.columbia.edu/SOURCES/.NOAA/.NGDC/.GLOBE/.topo/>).

stable isotopes of oxygen ( $\delta^{18}\text{O}$ ) and hydrogen ( $\delta^2\text{H}$ ) and their derivative d-excess, which together can provide information on temperature and on moisture sources and transport. Stable isotopes from ice cores drilled throughout the TP have been used to reconstruct climate histories extending back several thousands of years (Thompson et al., 2005); however, the interpretation of these isotopes is not yet fully resolved.

Since 1984 ice cores have been recovered from five ice fields across the TP (Fig. 1A) by The Ohio State University's Byrd Polar and Climate Research Center (OSU-BPCRC), in collaboration with the Lanzhou Institute of Glaciology and Geocryology (LIGG) and the Chinese Academy of Science's Institute of Tibetan Plateau Research (ITP-CAS). Each core has provided new information about climatic and environmental changes on regional to hemispheric scales (e.g., Beaudon et al., 2017; Duan et al., 2007; Sierra-Hernández et al., 2018; Thompson et al., 1989, 1990, 1997, 2000, 2005, 2006a,b, 2011; Tian et al., 2006; Yao et al., 1997, 2006). Taken together, these records demonstrate the TP's climatic complexity and diversity. One of the ice fields, the Guliya ice cap (35.13°N; 81.38°E; 6710 masl), covers 200 km<sup>2</sup> and is located in the western Kunlun Mountains (Fig. 1B), one of the longest mountain chains in Asia which extends from the Karakorum Range in the west to near the Qaidam Basin in the east. Guliya lies in the driest region of the TP above the highest equilibrium line altitude (Yao et al., 2012), and the current maximum accumulation (~230 mm water equivalent (w.e.)/year (a<sup>-1</sup>)) is the lowest of all the ice fields that have been drilled jointly by OSU-BPCRC and ITP-CAS. Reconnaissance field programs were conducted in 1990 and 1991, and a drilling program in 1992 resulted in the retrieval of a core to the bedrock on the Guliya Plateau (GP) (Fig. 1C). Twenty-three years passed before the site was revisited for another deep-drilling program.

Here we present and discuss recent climate records from ice

cores drilled in 2015 on Guliya and changes in temperature proxies and ice accumulation that have occurred across the ice cap since the mid-19th century. The cores have been analyzed at annual to subannual resolution for chemical and physical parameters, and the climate records from these analyses will be used to describe teleconnections among the western interior of the TP, the North Atlantic, the Arctic, and tropical oceans. The last 1000 years of the Guliya  $\delta^{18}\text{O}$  record from both the 1992 and 2015 GP cores, along with other ice core  $\delta^{18}\text{O}$  time series from around the TP (Fig. 1A), will be used to illustrate similarities and variations in the climate history of this region. Finally, the recent warming trend across the TP will be evaluated using stable isotopic time series from the ice cores.

## 2. Materials and methods

In 1990 and 1991, a cooperative team from the OSU-BPCRC and the LIGG recovered several short cores from the Guliya ice cap, including a 16 m firn core in April 1991 from the Guliya Summit (GS) at 6710 m above sea level (masl) (Fig. 1C), along with samples from a 1.5 m pit (Fig. S1). Temperatures were measured in the shallow summit borehole (Fig. 2). The pit and shallow core samples were analyzed for  $\delta^{18}\text{O}$  and concentrations of mineral dust, and beta activity ( $\beta$ ) from <sup>90</sup>Sr and <sup>137</sup>Cs decay was measured in the top 5 m of the core to identify the 1962/63 Arctic thermonuclear test. The  $\delta^{18}\text{O}$  stratigraphy of the pit (<sup>18</sup>O depletion in winter and enrichment in summer) is consistent with polar cores and opposite to that in the Dasuopu glacier in the central Himalaya (28°N; 85°E) which is located directly within the ISM influence (Thompson et al., 2000). However, seasonal dust concentrations in the pit are consistent with Dasuopu (i.e., high in the winter and early spring and low in summer). The sample handling of the Guliya 1991 pit

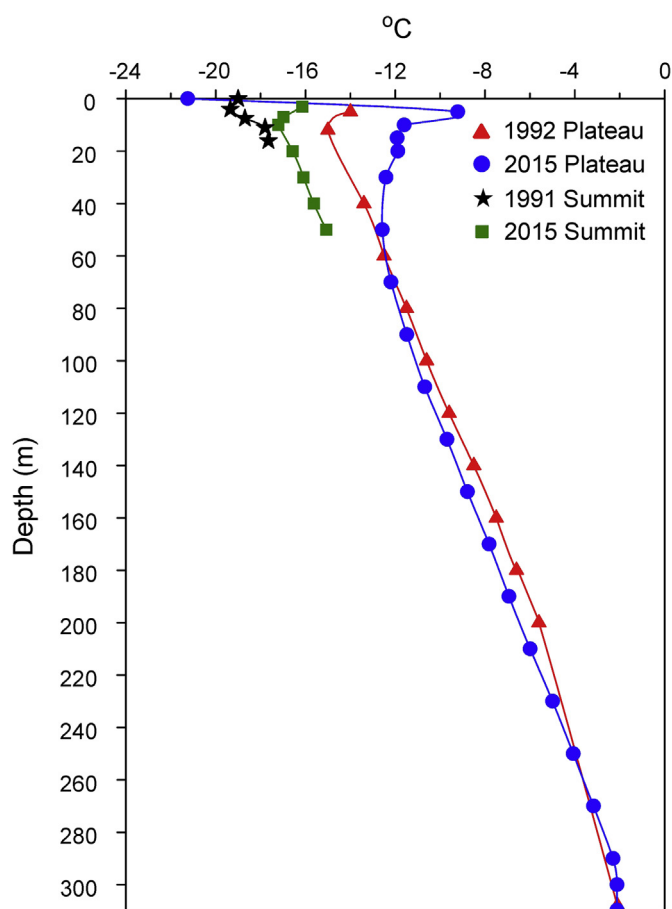


**Fig. 2.** Guliya borehole temperatures. Borehole temperatures ( $^{\circ}\text{C}$ ) on Guliya Summit in 1991 (black stars) and 2015 (green squares), Guliya Plateau in 1992 (blue closed circles), and Guliya Plateau in 2015 (red triangles).

may have affected the dust concentrations, since the samples were melted and bottled on site.

In 1992 a 308.6 m core (1992PC) was drilled to bedrock on the GP (6200 masl) below the summit (Fig. 1C), and a 90 cm snow pit was excavated and sampled near the borehole. Unlike the 1991 GS pit samples, those from the 1992 GP pit were returned frozen to the OSU-BPCRC labs. The analysis of the pit shows one annual cycle in  $\delta^{18}\text{O}$ , mineral dust and chloride (Fig. S1), and the isotopic and aerosol seasonal variations are similar to those in the 1991 summit pit. Subsequent to the drilling of the 1992 plateau core (1992PC) a borehole temperature profile was produced which showed a bottom temperature of  $-2.1^{\circ}\text{C}$ , confirming that the ice was frozen to the bed (Fig. 2). The visible core stratigraphy was characterized by light to dark brown dust layers. As this core was split equally along its entire length between the OSU-BPCRC and the LIGG, each team received a sub-optimal amount of ice on which to perform all their analyses. The OSU-BPCRC half-core was measured continuously at high resolution (average sample length of 2.4 cm) for  $\delta^{18}\text{O}$  and concentrations of chloride ( $\text{Cl}^{-}$ ), nitrate ( $\text{NO}_3^{-}$ ), sulfate ( $\text{SO}_4^{2-}$ ) and mineral dust, and  $\beta$  was analyzed in the top 10 m of a 34-m core drilled adjacent to the deep borehole. Chlorine-36 ( $^{36}\text{Cl}$ ) analyses performed at intervals throughout the core indicate very old ( $>500$  ky) basal ice (Thompson et al., 1997). However, because the original amount of ice was so limited, the lowest 20 m of the archive is depleted. This, along with the limitations of the techniques for dating old ice two decades ago, complicated efforts to confirm the age of the basal ice and thus establish a firm chronology for the bottom of 1992PC.

From September to October of 2015 teams from the OSU-BPCRC and the ITP-CAS revisited the Guliya ice cap for the first time since 1992 in order to drill a new core to bedrock on the GP close to the location of original drill site. A further objective was to recover cores to bedrock on the GS, which was not achievable 23 years earlier due to logistical limitations. The accomplishments of the recent expedition include a core to bedrock (309.73 m) and an adjacent core (72.40 m) from the GP and three cores to bedrock (50.72 m, 51.38 m, 50.86 m) from the GS. As in 1992, the shorter plateau core (2015PC1) and long plateau core (2015PC2) were split equally along their lengths between the OSU-BPCRC and the ITP-CAS. The ITP-CAS received the entire first summit core (2015SC1), the OSU-BPCRC received the entire third summit core (2015SC3), and the second (2015SC2) was split along its length between the two institutions. Temperatures were measured in the 2015PC2 and 2015SC1 boreholes (Fig. 2), which confirm that the ice is frozen to the bed at both sites although temperatures in the upper sections diverge from those in the earlier profiles as discussed in Section 3.

Similar to the 1991 GS and 1992 GP cores, the analyses of the new Guliya cores include  $\beta$ ,  $\delta^{18}\text{O}$ , concentrations and size distributions of mineral dust, and concentrations of  $\text{Cl}^{-}$ ,  $\text{NO}_3^{-}$  and  $\text{SO}_4^{2-}$ . In addition, analyses of the new cores include  $\delta^2\text{H}$ , and concentrations of sodium ( $\text{Na}^{+}$ ), ammonium ( $\text{NH}_4^{+}$ ), potassium ( $\text{K}^{+}$ ), magnesium ( $\text{Mg}^{2+}$ ), calcium ( $\text{Ca}^{2+}$ ), and fluoride ( $\text{F}^{-}$ ). Future analyses will include  $^{14}\text{C}$  on organic material trapped in the ice, and  $^{36}\text{Cl}$ , beryllium-10 ( $^{10}\text{Be}$ ),  $\delta^{18}\text{O}$  of air in bubbles trapped in the ice, and argon isotopic ratios ( $^{40}\text{Ar}/^{38}\text{Ar}$ ) on deep sections of 2015PC2 to determine more precisely the age of the ice cap.

Reconstructing annually-resolved time series in the upper sections of the Guliya cores is complicated by the very low annual accumulation and post-depositional effects such as wind scour. Unlike the GP, which is entirely composed of ice below  $\sim 1$  m from the surface, the GS contains a 24.5 m firn pack which reflects the much colder conditions at this elevation that allow loose snow to persist. The development of annual time scales for the GP cores is discussed in the supplement (Figs. S2 and S3).

### 3. Guliya's record of recent climate change

Tian et al. (2001) and Yao et al. (2013) divide the TP into three climate domains based on precipitation rate and the seasonal variations of  $\delta^{18}\text{O}$  in precipitation: the westerlies-dominated latitudes north of  $34^{\circ}$  to  $35^{\circ}\text{N}$ , the monsoon-dominated southern tier (south of  $31^{\circ}$  to  $32^{\circ}\text{N}$ ), and the transition between them (Fig. 1A). The spatial distribution and stable isotopic chemistry of summer precipitation along the southern and southeastern periphery of the TP is driven primarily by the Southeast Asian monsoon and the ISM (Tian et al., 2001). However, the direct influences of the monsoons diminish toward the arid interior of the Third Pole. The northern TP is subject to transient influences from at least two large-scale atmospheric circulation systems: continental westerly cyclogenesis during the winter and spring and the monsoons in summer via convective moisture recycling (Davis et al., 2005; Dong et al., 2016; Tian et al., 2001, 2007; Yao et al., 2012). The Southern Oscillation in the tropical Pacific is also suggested to have an indirect influence on the climate in this region (Wang et al., 2003).

Controls over precipitation in arid western Tibet are not as well understood as they are over the eastern and southern TP. The location of the Guliya ice cap in the interior of the Asian continent at such a high elevation and so far from the south Asian moisture sources ensures very low annual precipitation, a significant portion of which is delivered by westerly cyclogenesis with nearly half resulting from local moisture recycling (An et al., 2017). Precipitation in the western Kunlun Mountains is seasonal, although less so than in the monsoon regions to the south. Summertime (June to

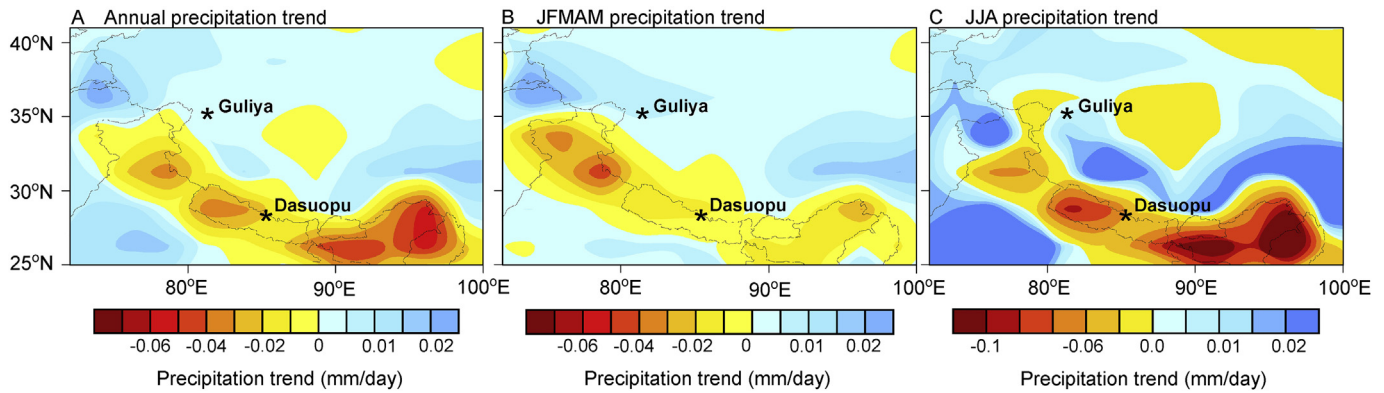


**Fig. 3. Precipitation rate trends (1979–2014) across northern India and western TP.** Trends of (A) annual precipitation rate (mm/day) show similar regional patterns to both (B) winter/spring (January to May) and (C) summer (June to August) trends, although the decreasing summer trend in the Himalaya is greater. The locations of the Guliya and Dasuopu ice fields are noted. Data used to map the trends are from the Global Precipitation Climatology Project ([www.esrl.noaa.gov/psd/data/gridded/data.gpcp.html](http://www.esrl.noaa.gov/psd/data/gridded/data.gpcp.html)).

August) snowfall accounts for ~45% of the annual total, while the amount from January to May accounts for ~35% (Fig. S4). The lowest amount falls in the autumn (September to December). Distinctive trends in recent years (1979–2014) in annual and seasonal precipitation rates throughout the TP are illustrated in Fig. 3(A–C). The increasing aridity in the Himalaya is most obvious, with the greatest rate of precipitation decrease occurring during the summer monsoon (JJA) season. On the other hand, the western Kunlun Mountains to the north received slightly more winter/spring (January to May, or JFMAM) and summer precipitation over this period. In particular, precipitation around Guliya has increased at approximately the same rates in JFMAM (Fig. 3B) and JJA (Fig. 3C). The opposing trends in annual precipitation rates between the Himalaya and the TP regions to the north are reflected on longer time scales in TP ice core net balance records since 1600 CE, which show opposite decadal-scale trends between Dasuopu in the monsoon-dominated south and Guliya, Puruogangri, and Dundu in the westerlies-dominated and transition regimes (Thompson et al., 2006a).

The high degree of reproducibility between the  $\delta^{18}\text{O}$  profiles from cores drilled in the early 1990s and those drilled in 2015 (Fig. 4) allows assessment of the climate changes in the western Kunlun over the last half-century. Matching of  $\delta^{18}\text{O}$  in the GP cores (Fig. 4A) shows that the top of 1992PC corresponds to 6.0 m depth in 2015PC1, which yields in an average annual layer thickness ( $LT_{\text{avg}}$ ) of 261 mm from 1992 to 2015. Beta activity from the early 1960s Arctic atmospheric nuclear bomb tests calibrates the 1962/63 horizon at ~10.9 m (Fig. S2B), which isotopically matches the 1992PC core at ~6 m resulting in a  $LT_{\text{avg}}$  of 200 mm from 1963 to 1992. Thus, the  $LT_{\text{avg}}$ , which is considered as a proxy for annual net balance on the GP, increased by ~30% from the earlier to the later period. Similar comparisons are made between 2015SC3 and 1991SC, the 16 m summit core drilled in 1991 (Fig. 4B); however, because all of the 1991SC and the top ~25 m of 2015SC3 are composed of firn, their  $\delta^{18}\text{O}$  stratigraphic profiles were converted to ice equivalent (i. eq.) depths in order to facilitate direct comparisons with the GP cores. Thus, an increase in  $LT_{\text{avg}}$  from 1991 to 2015 (125 mm i. eq.  $\text{a}^{-1}$ ) is observed relative to the previous 29 years (69 mm i. eq.  $\text{a}^{-1}$ ). It is apparent that the overall  $LT_{\text{avg}}$  at the summit is much lower than on the plateau; however, the increase of 81% in layer thickness between 1963–1991 and 1992–2015 on the GS is ~2.7 times that on the lower elevation GP site.

Many observations of recent TP climate show that temperatures have been rising over the 20th and into the 21st centuries (Li et al., 2010; Liu and Chen, 2000; Pepin et al., 2015). The temperature

variations on the Guliya ice cap are consistent with the trends on the TP, and this warming can be demonstrated both physically and isotopically. Borehole temperatures measured on the GP in 1992 and 2015 are similar below ~50 m but diverge above that depth (Fig. 2). Ice from ~5 to ~30 m depth in the 2015 borehole was warmer than ice measured in 1992 over the same depth interval, with the greatest differences occurring between 5 and 10 m (4 °C difference at 10 m, ~6–7 °C difference at 5 m depth). Note that the 2015 GP profile begins at the surface where temperatures are much colder than below, while the 1992 profile begins at 5 m depth. Similar to the GP, summit temperatures from the surface to ~10 m depth were lower in 1991 than in 2015 (Fig. 2).

The warming that is observed in the borehole measurements are confirmed by the stable isotopic chemistry of the ice. Several studies have demonstrated that  $\delta^{18}\text{O}$  is a reasonable proxy for surface and near-surface temperatures over northern Tibet on interannual time scales (Thompson et al., 2006a; Tian et al., 2003, 2006; Yao et al., 1996, 2013). Comparisons of the  $\delta^{18}\text{O}$  data in the top sections of 2015PC1 and 1992PC between 1963/1992 and 1993/2015 (Fig. 4A) in a similar manner to the  $LT_{\text{avg}}$  calculations described above demonstrate that on the GP the ice is isotopically enriched by 1.9‰ (from an average of –13.1‰ in 1963–92 to –11.2‰ in 1993–2015) as is the firn on the summit (from an average of –11.6‰ in 1963–1991 to –9.7‰ in 1991–2015). A paradox is presented by the higher  $\delta^{18}\text{O}$  values in the GS cores compared to those from the GP which is 500 m lower, particularly as borehole temperatures are lower on the summit (Fig. 2). The  $^{18}\text{O}$  enrichment on the GS possibly reflects more intense winter and spring winds (Fig. S5) which may remove unconsolidated,  $^{18}\text{O}$ -depleted snow. On the GP,  $\delta^{18}\text{O}$  values are “locked in” very quickly as surface snow turns to ice within a year, although this process may tend to smooth the seasonal isotopic variations (Fig. S2) that are easily discernible in the snow pit stratigraphy (Fig. S1). The quick conversion to ice may prevent vapor diffusion after deposition, thereby better preserving the interannual isotopic variations.

Annual averages of 2015PC1 and 2015PC2  $\delta^{18}\text{O}$  since 1961 (Fig. 5A), along with a continuous temperature record from Shiquanhe (32.5°N; 80°E; 4255 masl) (Fig. 5B) 320 km southwest of Guliya (Fig. 1A) and a West Himalaya minimum temperature record (Fig. 5C) show increasing trends until the mid-2000s, after which Shiquanhe temperature levels off as  $\delta^{18}\text{O}$  values decrease. While the average Guliya  $\delta^{18}\text{O}$  increased by 1.9‰ between 1963–1992 and 1993–2015 (Fig. 4), the Shiquanhe annual temperature increased by 1.4 °C between these periods. Although the West Himalaya minimum temperature record ends in 2007, an increase of 0.9 °C

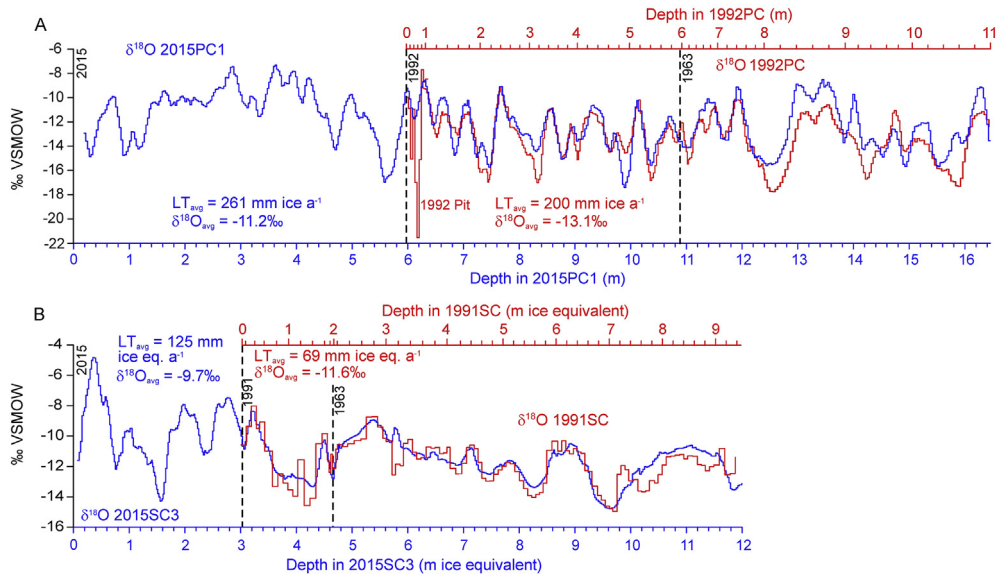


**Fig. 4.** Comparisons between early 1990s and 2015 Guliya records.  $\delta^{18}\text{O}$  matching between (A) 2015PC1 and 1992PC (both smoothed with 5-sample running means) and (B) 2015SC3 (smoothed with 5-sample running means) and 1991SC (not smoothed), demonstrating how temporal calibration points are established. Average annual layer thicknesses ( $LT_{avg}$ ) and  $\delta^{18}\text{O}$  shown in blue are calculated from the 2015 cores in both (A) and (B), while those shown in red are calculated from the early 1990s cores. The GP cores are composed of ice throughout their lengths (i.e., no firn), while the GS  $\delta^{18}\text{O}$  records are adjusted for density and are shown on ice equivalent depth scales.

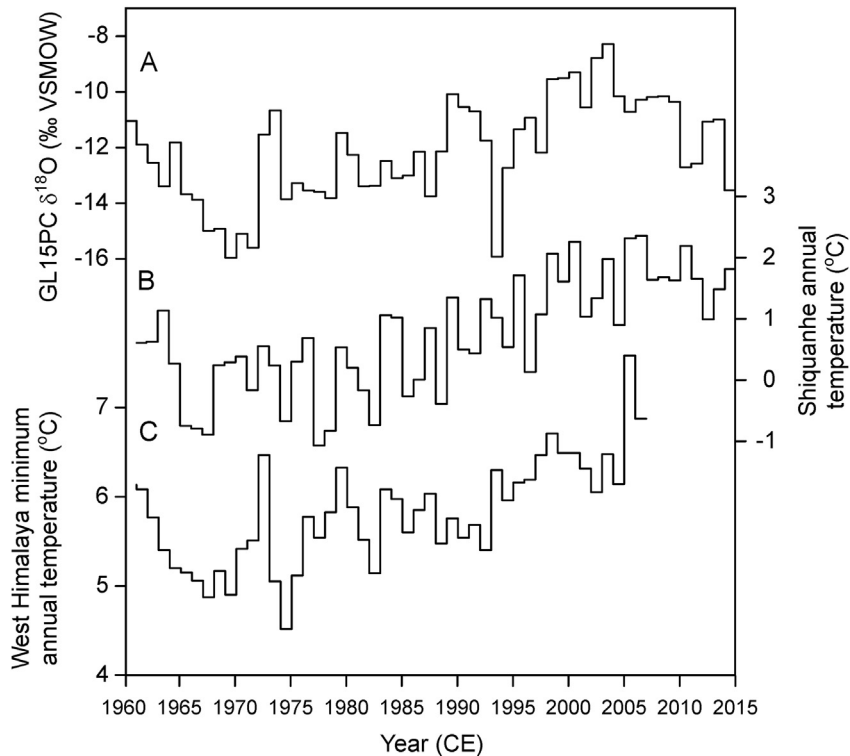


**Fig. 5.** Guliya  $\delta^{18}\text{O}$  and instrumental temperature records. (A) Annual GP  $\delta^{18}\text{O}$  (average of PC1 and PC2) compared with (B) annually averaged temperature data from Shiquanhe (320 km to the southwest of Guliya), and (C) annually averaged West Himalaya minimum temperatures. West Himalaya temperature data are from Homogeneous Indian Monthly surface temperature data sets provided by the Indian Institute of Tropical Meteorology (<http://www.tropmet.res.in/>), and the Shiquanhe temperature data are provided by the ITP-CAS.

between the periods most likely accounts for much of the recent warming. Assuming a  $\delta^{18}\text{O}$ -temperature conversion factor of  $0.62\text{‰}/\text{°C}$  in the northern TP (Yao et al., 2013), the temperature change between 1963–1992 and 1993–2015 at Guliya is calculated as  $3.1\text{°C}$ , which is  $1.7\text{°C}$  more than the change in the Shiquanhe

record. Elevation-dependent warming may be responsible for this much larger shift in the ice core time series. This phenomenon is well documented on the TP (Pepin et al., 2015), where instrumental records show greater warming with altitude from 1991 to 2012 compared with 1961–1990. The correlation coefficients between

the  $\delta^{18}\text{O}$  - Shiquanhe and  $\delta^{18}\text{O}$  - West Himalaya temperatures are highly significant ( $R = +0.48$ ,  $p < 0.01$ ;  $+0.57$ ,  $p < 0.01$ , respectively), although the positive trends drive the correlations. The two instrumental records report temperatures in areas that are more monsoon-dominated than the western Kunlun Mountains, and the ice core  $\delta^{18}\text{O}$  values may have been influenced to some degree by meteorological factors other than temperature, as well as by post-depositional modifications.

Time series of selected parameters from the top sections of the GP cores (dated to 1840 CE) are presented in Fig. 6 as 5-year running means. The  $\delta^{18}\text{O}$  and d-excess records (Fig. 6A and B) are composed of the averages of 2015PC1 (0–30.4 m) and 2015PC2 (0–34.1 m). The time series are shown individually in the supplemental information (Fig. S6). The positive  $\delta^{18}\text{O}$  trend (Fig. 6A) implies that climate in the western Kunlun region has been warming since the end of the Little Ice Age in the mid to late 19th century, with the greatest warmth occurring in the 1940s and around the 1990s to the early 2000s CE. The similarly increasing trend in d-excess (Fig. 6B) may provide information about the sources of the precipitation and the transport pathways. For example, d-excess

has been linked with monsoon precipitation intensity in the central Himalaya (Thompson et al., 2000). Higher values in the Dasuopu ice core record are coincident with lower net balance (a proxy for precipitation) on decadal to centennial time scales, and together these suggest that the ISM circulation in the central Himalaya has weakened since the mid-19th century. The trends of both the Guliya and Dasuopu d-excess time series increase from 1840 to 1997 CE (0.17‰/decade for Dasuopu, 0.10‰/decade for Guliya), although their primary moisture sources differ. However, since 1979 the JJA precipitation rate in the central Himalaya where Dasuopu is located has decreased more than the winter/spring rate (Fig. 3B and C). This decrease in the summer/winter ratio in annual snowfall may partially control the d-excess increase in Dasuopu, since on the southern TP low d-excess is driven by monsoon precipitation (Tian et al., 2007). Over the same period, the rates of precipitation from winter continental and summer recycled moisture sources have increased in the western Kunlun and on Guliya (An et al., 2017), although the summer/winter ratio may have remained constant on Guliya but has decreased around the ice field. In the northwestern TP, summer (winter) moisture is characterized

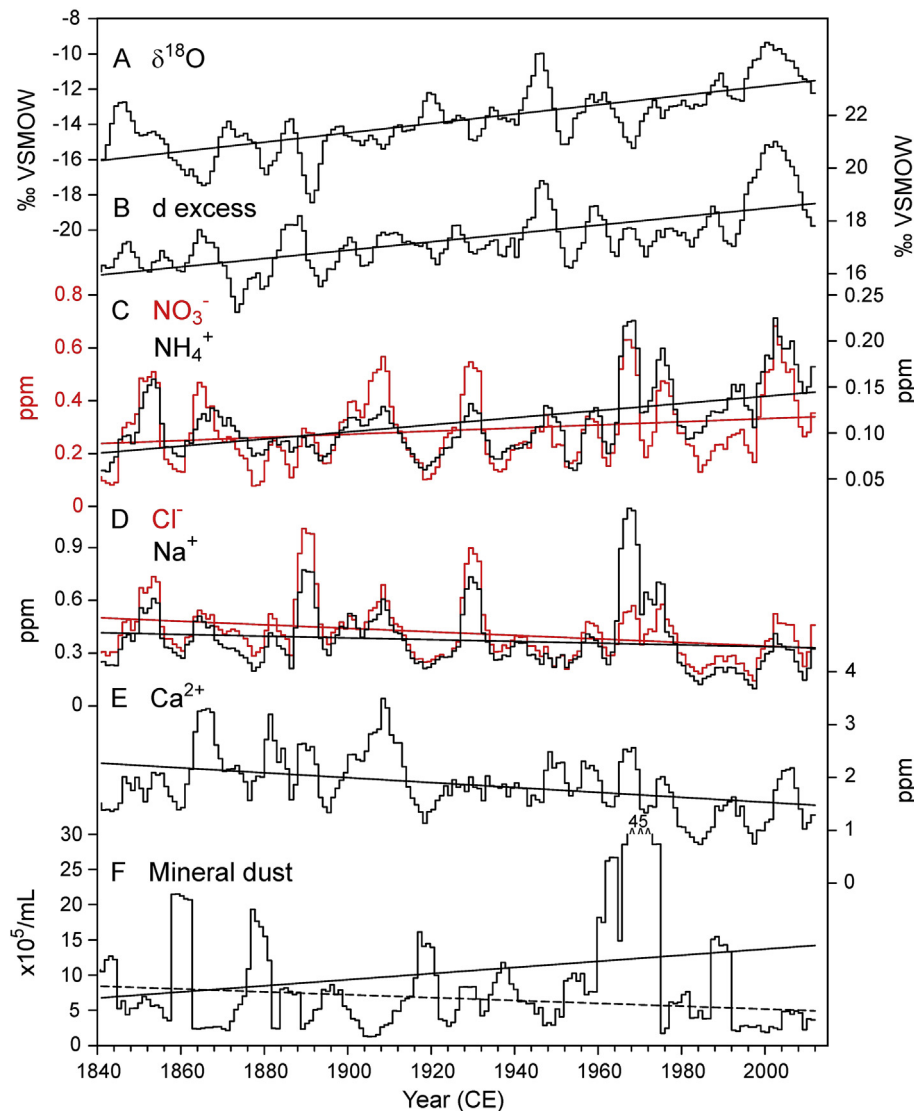


**Fig. 6.** Guliya ice core chemistry and dust records since 1840 CE. Time series from GP covering the period 1840 to 2014 (5-year running means) of (A)  $\delta^{18}\text{O}$  (average of 2015PC1 and PC2), (b) deuterium excess (average of 2015PC1 and PC2), and 2015PC1 concentrations of (C) nitrate and ammonium, (D) chloride and sodium, (E) calcium, and (F) mineral dust (0.63–16  $\mu\text{m}$  diameters). All plots are shown with 1st order polynomial trends lines. In (F) the dashed trend line pertains to data excluding the 1961 to 1975 dust peak.

by higher (lower)  $\delta^{18}\text{O}$  and lower (higher) d-excess (Tian et al., 2007). Tree ring studies in the Karakorum mountain range in northern Pakistan west of Guliya indicate that 20th century winter precipitation was the highest of the last millennium, which is attributed to an intensification of the hydrological cycle in central Asia (Treydte et al., 2006). The Karakorum has a more Mediterranean-type climate (higher winter than summer precipitation) than the western Kunlun, although winter precipitation in this region extends into the western TP.

Lake levels in Central Asia and across the TP also indicate that the climate north of the monsoon domain, including the Kunlun Mountains, has become wetter since the middle of the 20th century in response to strengthening westerlies and warming climate (Fang et al., 2016; Lei et al., 2014). This increasing winter precipitation may explain the opposing trends in  $\text{NO}_3^-$  and  $\text{NH}_4^+$  (Fig. 6C) versus  $\text{Cl}^-$ ,  $\text{Na}^+$  and  $\text{Ca}^{2+}$  (Fig. 6D and E) concentrations in 2015PC1. The  $\text{NO}_3^-$  and  $\text{NH}_4^+$  in the Guliya ice may have biological origins potentially linked to lake expansion (Wang et al., 2006) and/or Central Asian anthropogenic sources (Zhao et al., 2011). The decreasing trends in the lithic and salt-derived ions possibly result from shrinking source areas, also a function of local and upwind lake expansion. Mineral dust concentrations in 2015PC1 show quasi-periodic (~20 year) oscillations with a sharply defined peak from ~1960 to ~1975 (Fig. 6F) suggestive of increased dust storm frequency and/or intensity, although since the middle of the 20th century the frequency of dust storms across northern China has decreased (Qian et al., 2002). The general trend of the dust concentrations is positive (solid line in Fig. 6F), but if the late 20th century peak is removed the trend turns negative (dashed line). After 1975, concentrations of  $\text{Cl}^-$ ,  $\text{Na}^+$ ,  $\text{Ca}^{2+}$ , and mineral dust decreased abruptly compared with 1840–1975 levels (–27%, –39%, –34%, respectively) as  $\text{NO}_3^-$  and  $\text{NH}_4^+$  increased (+19%, +45%, respectively), which is coincident with increased regional lake expansion in Central Asia (Lei et al., 2014) and the Kunlun Mountains (Fang et al., 2016) and enhanced moisture recycling (An et al., 2017).

#### 4. Large-scale oceanic and atmospheric influences on Guliya precipitation

##### 4.1. North Atlantic influence on the ISM and western Kunlun Mountains

As noted above, over the last half century the GP  $\delta^{18}\text{O}$  record shares similarities with regional surface temperatures (Fig. 5). On a much broader scale, this GP isotope/temperature association extends into the Arctic (Fig. 7A–D) and throughout China (Fig. S7). All the time series in Fig. 7(A–D) are detrended and filtered with 19-year moving averages to emphasize decadal-scale variations without the dominant long-term trends. The temperature record from Greenland (Fig. 7B) (Box et al., 2009) is derived from instrumental records and climate modeling, and the  $\delta^{18}\text{O}$  ice core record from Graham Bell Island in Franz Josef Land (81°N; 64°E) (Fig. 7C), is interpreted by Henderson (2002) as a winter temperature proxy. Both records are very similar to the Arctic zonal temperature anomalies (Fig. 7A) such that cool/isotopically depleted periods occurred from ~1880 to 1920 CE and ~1960 to ~1980 CE, while warming/isotopic enrichment is evident from the 1940s to the 1960s and after the early 1980s. The decadal-scale similarities between the Arctic temperature records and temperature proxies and the GP  $\delta^{18}\text{O}$  record (Fig. 7D) suggest a link between the climate regimes of the high latitudes and this region of Eurasia, including the western Tibetan Plateau. Linkages have been investigated among the North Atlantic Oscillation (NAO) (Hurrell, 1995, 1996), the Arctic Oscillation (Rigor et al., 2000) and the strength of the

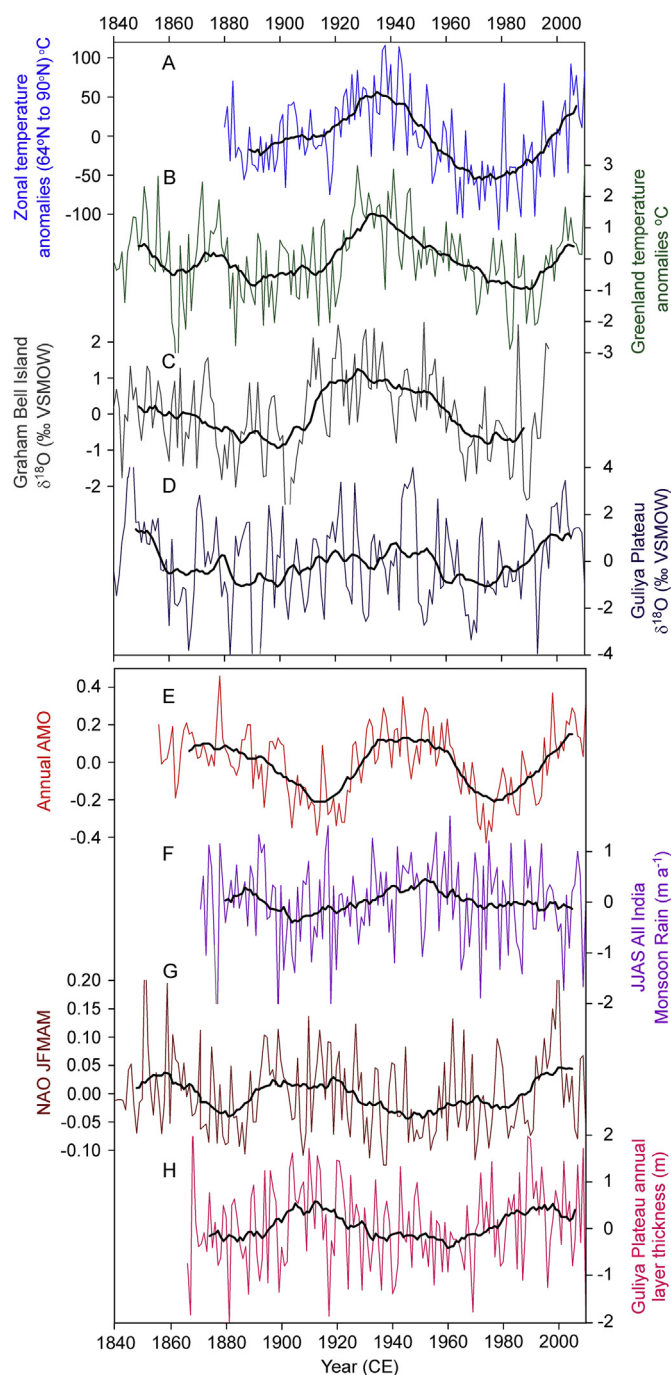


**Fig. 7. Teleconnections between Guliya, the North Atlantic and the Indian summer monsoon.** (A) Zonal temperature anomalies from 64°N to 90°N (GHCN-v3 1880–07/2017 + SST: 1880–07/2017 ERSST v5); (B) Greenland ice sheet land station temperature anomalies (Box et al., 2009); (C)  $\delta^{18}\text{O}$  time series from the Graham Bell Island ice core, Russian Arctic (Henderson, 2002). These Arctic temperature records are compared with (D) GP  $\delta^{18}\text{O}$  data from 1840 to 2014 (average of 2015PC1 and 2015PC2); (E) Annually averaged Atlantic Multidecadal Oscillation index (<https://www.esrl.noaa.gov/psd/data/timeseries/AMO/>); (F) the all India monsoon rainfall from June to September, from the Indian Institute of Tropical Meteorology website ([http://www.tropmet.res.in/static\\_page.php?page\\_id=53](http://www.tropmet.res.in/static_page.php?page_id=53)); and (G) the average January to May Hurrell Station based North Atlantic Oscillation Index (<https://climatedataguide.ucar.edu/climate-data/hurrell-north-atlantic-oscillation-nao-index-station-based>) are compared with (H) the GP layer thickness record, which is the average of 2015PC1 and 2015PC2. All time series are smoothed with 19-year moving averages, and A to D, F and H are detrended. The unsmoothed, detrended data for the plots are shown behind their spline curves.

Siberian High (Gong and Ho, 2002), a strong winter anticyclone which moves cold air from the Arctic southward toward the Eurasian mid-latitudes. Riaz et al. (2017) suggest that the intensity of the Siberian High is an important factor for winter temperatures in their study region, which includes the high mountain regions of the Karakorum, the western Himalaya and the western Kunlun Mountains.

Links between atmospheric circulation and sea surface temperatures (SSTs) in the North Atlantic region and the strength of the ISM on decadal to millennial time scales have been extensively researched (e.g., Chang et al., 2001; Goswami et al., 2006; Gupta et al., 2003; Mohtadi et al., 2014). Decadal-scale similarities are illustrated in Fig. 7(E, F) between the Atlantic Meridional Oscillation (AMO) (Schlesinger and Ramankutty, 1994) and the all-India monsoon rainfall (AIMR), which was also noted by Feng and Hu (2008). Wang et al. (2014) proposed that these variations between the North Atlantic and the ISM are connected by a mechanism in which warming of the North Atlantic (positive AMO) forces warming of the TP, illustrated by the GP  $\delta^{18}\text{O}$  record (Fig. 7D) and a composite China temperature record (Fig. S7) developed by Wang and Gong (2000). This landmass warming enhances the meridional temperature gradient between the warm, high massifs and the relatively cooler Indian Ocean, thus stimulating the monsoon circulation (Feng and Hu, 2008). Atmospheric circulation changes related to the NAO (Fig. 7G) affect the extent of the impact of the AMO on the ISM. It is interesting to note that the positive relationships between the AIMR index and the AMO discontinue after the late 1970s. Wu (2005) proposed that the ISM has weakened over recent decades, possibly because of the weakening of the land-sea thermal gradient as the rate of warming has increased in the Indian Ocean (Roxy et al., 2015).

The GP annual layer thickness (LT) record (Fig. 7H) provides a decadal-scale indication of snowfall amount in the western Kunlun Mountains. These LTs have not been corrected for thinning with depth, which is minimal in the upper 30–35 m of the GP cores (Fig. S3A); however, the time series is detrended, which de-emphasizes the layer thinning. The relationships among the variations of the GP LT, the AMO and AIMR are such that low (high) GP LT corresponds with high (low) North Atlantic SSTs and high (low) Indian monsoon rainfall. However, the GP LT varies synchronously with the average January to May (JFMAM) NAO (Fig. 7G). A similar relationship between the North Atlantic atmospheric circulation and TP snow depth was observed by Xin et al. (2010), who noted that years of positive winter NAO coincide with increased snow depth, perhaps through the intensification of the Asian tropical westerly jet which extends from the tropical Atlantic through northern Africa and the Middle East to the southwestern TP. Archer and Fowler (2004) observed a significant positive correlation between winter NAO and winter precipitation measured in the Karakorum Mountains, and precipitation in Central and High Asia is also linked to North Atlantic SSTs (Chen et al., 2008).

The increase (decrease) in snow depth as inferred by the GP LT record (Fig. 7H) may weaken (strengthen) the meridional temperature gradient between the TP and the Indian Ocean and thus weaken (strengthen) the ISM, as indicated by the AISM rainfall (Fig. 7F). On decadal time scales the JFMAM NAO - AISM and AISM - GP LT are significantly correlated ( $R = -0.64$  and  $-0.71$ , respectively,  $p < 0.01$  for both), and Goswami et al. (2006) link the NAO to the monsoon through modulation of the tropospheric meridional temperature gradient over Eurasia. The linkages between TP snow depth and/or snow cover during the winter and spring and the strength of the ISM during the following summer have long been hypothesized (Blanford, 1884; Ge et al., 2017; Walker, 1910; Wu and Qian, 2003; Zhao and Moore, 2004), and are consistent with the relationships illustrated in Fig. 7(F, H). The rapid rate of LT increase

after 1975, which is coincident with the leveling of the AISM index, appears to agree with the analysis of Xin et al. (2010) which points to a weakening of the monsoon as the winter snow depth increased beginning in the late 1970s and the land/sea thermal gradient decreased (Roxy et al., 2015). This increase, at least in the eastern TP, is attributed to the Northern Hemisphere climatic reorganization of the mid-1970s (Trenberth and Hurrell, 1994), which was concomitant with intensification of: (1) the subtropical westerly jet; (2) the southerly moisture flow over the Bay of Bengal; (3) the ascending air over the TP; and (4) the India-Burma trough (Zhang et al., 2004).

#### 4.2. Indian summer monsoon influence on the western Kunlun Mountains

Sediment cores from Taro Co ( $31^\circ\text{N}$ ;  $84^\circ\text{E}$ ) provide evidence that the northern boundary of the ISM influence shifted northward rapidly as the Little Ice Age ended in the mid-19th century (Zhang et al., 2017) due to increasing land/sea thermal contrast as the TP heated, which is consistent with the increasing  $\delta^{18}\text{O}$  in the Guliya record (Fig. 6A). Dong et al. (2016) proposed that under the current climate, precipitation from intrusive convective storms that originate in central eastern India may extend into the southwestern region of the Third Pole (SWTP) through mid-tropospheric circulation. Middle and upper level (300 hPa) circulation transports convectively-lifted moisture over the Himalaya onto the SWTP. The movement of moisture from north central India to the TP is characterized by two types, upslope transport (“non-intrusive”), which is more frequent but less efficient, and “up and over”, or “intrusive” transport, which is less frequent but more efficient and accounts for approximately half of the total summer precipitation over the SWTP (Dong et al., 2016). This intrusive storm precipitation is often followed by local convection which peaks in the afternoon. Tian et al. (2007) consider Shiquanhe at  $32.5^\circ\text{N}$  to be located in the area currently under monsoon influence which is affected by intrusive convective storm events as demonstrated by Dong et al. (2016), although Yao et al. (2013) place it within the westerlies-monsoon transition regime (Fig. 1A). According to all the criteria discussed here, under current climate conditions the Guliya ice cap is located within the westerlies-dominated regime, although in close proximity to its southern boundary. It is possible that recycled moisture from intrusive convection (characterized by lower  $\delta^{18}\text{O}$  and d-excess values) that falls on the TP to the south of Guliya may reach the ice cap. Indeed, Ramisch et al. (2016) discovered lacustrine evidence in the Kunlun Mountains that placed the northern boundary of the monsoon as far as  $36^\circ\text{N}$  during the Holocene, and suggest that changes in monsoon strength can have impacts on the location of this boundary. Interestingly, the GP stable isotope records (Fig. 6A and B) show that from 1924 to 2012 CE the  $\delta^{18}\text{O}$  and d-excess are significantly correlated ( $R = 0.86$ ,  $p < 0.01$ , 5-year running means), but before 1925 the correlation is not significant ( $R = 0.11$ ,  $p > 0.3$ ). Obviously, more research is required to understand the controls on stable isotopes, and particularly on d-excess, in the cryosphere and the hydrosphere of this region of the TP.

#### 4.3. Tropical Pacific influence

Although precipitation chemistry and intensity in the western Kunlun Mountains are strongly influenced by the North Atlantic, linkages with the tropical Pacific are also evident. Yang et al. (2000) observed that 60 out of 87 El Niño years between 1690 and 1987 corresponded to negative net accumulation anomalies in the 1992 Guliya record. However, they found little relationship between El Niño and Guliya  $\delta^{18}\text{O}$ . The lack of correlation between Guliya  $\delta^{18}\text{O}$  and the eastern tropical Pacific is also illustrated in Fig. 8, which shows spatial correlation fields between 5-year running means of

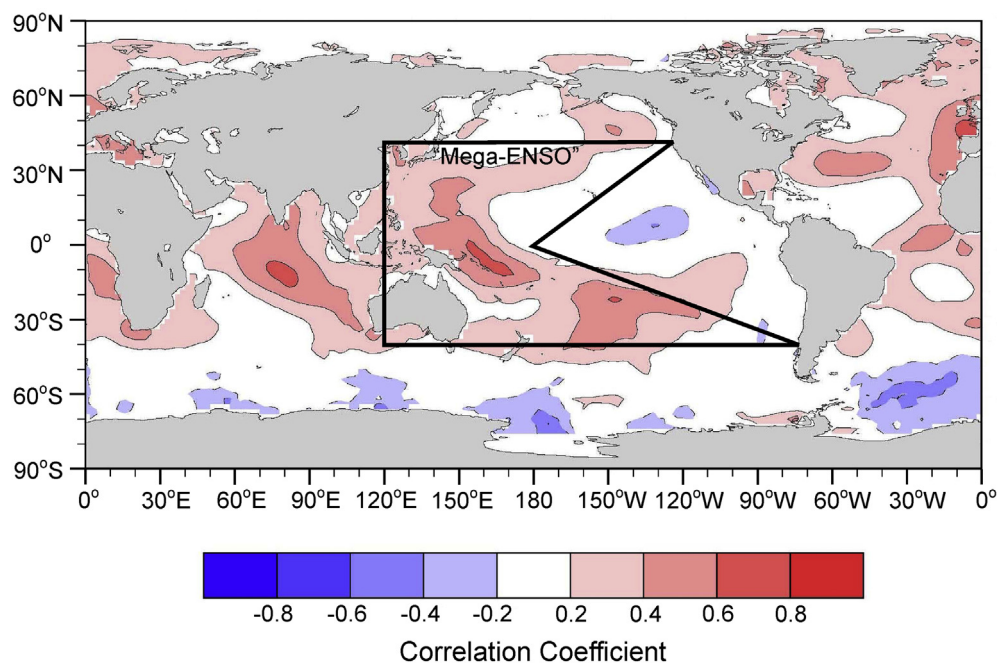


**Fig. 8. Teleconnections between Guliya and the tropical Pacific.** Correlation fields ( $p < 0.05$ ) between detrended, 5-year moving averages of NOAA annual extended reconstructed sea surface temperature (ERSST) data (v4) and similarly treated GP  $\delta^{18}\text{O}$  data from 1901 to 2012. The western portion of the “mega-ENSO” region defined by Wang et al. (2013) is outlined.

GP  $\delta^{18}\text{O}$  from the 2015 ice cores and similarly smoothed extended reconstructed SSTs (Huang et al., 2015; Liu et al., 2015) from 1901 to 2012. However, these correlations do show significant positive fields ( $p < 0.05$ ) in a region from the western equatorial Pacific to the northern and southern subtropical central Pacific, which coincides with a similarly shaped region of high SST anomalies (black outlined area in Fig. 8) defined by Wang et al. (2013) as the western component of a “mega-ENSO”. Significant correlations were noticed by Wang et al. (2013) between the “Northern Hemisphere summer monsoon”, or NHSM (of which the ISM is a component) and the mega-ENSO index (calculated as SST differences between expanded sections of the western and eastern Pacific). While the trend in ENSO has not changed over the last 30 years, the trends in both mega-ENSO and the GP  $\delta^{18}\text{O}$  have increased. Significant ( $p < 0.05$ ) correlation fields between GP  $\delta^{18}\text{O}$  and SSTs also occur in the Indian Ocean, the source region for a portion of the summer monsoon precipitation that ultimately recycles through the interior of the western TP, and in the North Atlantic which is consistent with the time series comparisons of GP  $\delta^{18}\text{O}$  and AMO (Fig. 7D and E). Wang et al. (2013) suggested that the SST anomalies in the North Atlantic associated with the AMO impact the Pacific SSTs and the NHSM precipitation and circulation.

### 5. Third Pole ice core climate records over the last millennium

Since 1987 the OSU-BPCRC, the LIGG and the ITP-CAS have collaborated in ice core drilling programs at four additional sites across the Third Pole: Dunde in 1987, Dasuopu in 1997, Puruogangri in 2000 and Naimona'nyi in 2006 (Fig. 1A). The majority of the precipitation arrives in JJAS at all the sites, including Guliya, although the lowest annual precipitation occurs in the north and the west. The region around Guliya receives the lowest precipitation of all the ice core sites, and the lowest percentage of summertime precipitation (Table 1).

Ice cores drilled throughout the TP over the last three decades

have provided climate records that show long-term similarities and short-term regional differences. Records of  $\delta^{18}\text{O}$  variations in ice cores from these five sites (Fig. 9), illustrated as 5-decade moving averages, are overlain by 6th order polynomial functions in order to demonstrate decadal to centennial-scale variations. Dunde (Fig. 9A) and Guliya (Fig. 9B) lie in the northern and westernmost regions of the TP, where the stable isotopes are influenced primarily by continental westerlies in spring and winter and moisture recycling via thermal convection in summer. Puruogangri (Fig. 9C) lies in the transition zone in the center of the TP. Tian et al. (2001, 2007) place it on the boundary between the continental and monsoon regimes based on the seasonality of  $\delta^{18}\text{O}$  variations in the precipitation. Puruogangri may also fall under the indirect influence of the SE Asian monsoon. Naimona'nyi (Fig. 9D) and Dasuopu (Fig. 9E) are both Himalayan sites and therefore receive more direct summer monsoon precipitation, although the former is located near the boundary between the monsoon and the transition regimes (Fig. 1A). Of all the TP  $\delta^{18}\text{O}$  records, the two from the Himalaya show the lowest average  $\delta^{18}\text{O}$  over the last millennium (Table 1).

Although similarities are apparent between  $\delta^{18}\text{O}$  time series from the same region (i.e., Dasuopu and Naimona'nyi are very similar, Dunde and Guliya show common large-scale features), little similarity is observed in the  $\delta^{18}\text{O}$  records between the southern and northern TP. The Himalayan and transition zone records display comparable  $^{18}\text{O}$  enrichment through the last millennium, which suggests that these regions either have been warming at a more consistent rate than the northern TP, or that the steadily increasing ISM strength had dampened the temperature effects of the isotopic variations over the past centuries. Monsoon intensity, inferred by the strengthening of monsoon winds over the Arabian Sea (Anderson et al., 2002) (Fig. 9F), has been increasing since the early 17th century. This is attributed to either centennial-scale warming over much of the TP, which may be responsible for the increase in the land/ocean thermal gradient (Feng and Hu, 2005, 2008), or forcing of Northern Hemisphere temperature by solar output, volcanic emissions, or greenhouse gas changes (Anderson et al., 2002).

**Table 1**  
Location and elevation for each of the 5 ice core drill sites on the TP. JJAS and annual precipitation (ppt) are from NASA GES-DAAC TRMM\_L3 TRMM\_3B42 v7 daily precipitation data (1998–2014 climatology); each JJAS and annual sum is from the grid point closest to the respective drill site. The  $\delta^{18}\text{O}$  means are based on the ice core records from each site as shown in Fig. 9.

	Location	Elevation masl	JJAS ppt mm	Annual ppt mm	% JJAS ppt a <sup>-1</sup>	$\delta^{18}\text{O}$ mean since 1000 CE
Dunde	38.13°N; 96.63°E	5325	157	212	74	-10.6
Guliya	35.13°N; 81.38°E	6200	78	133	50	-14.2
Puruogangri	33.88°N; 89.35°E	6070	166	235	71	-14.7
Naimona'nyi	30.38°N; 81.38°E	6050	297	468	63	-19.5
Dasuopu	28.38°N; 85.88°E	7200	697	969	72	-20.3

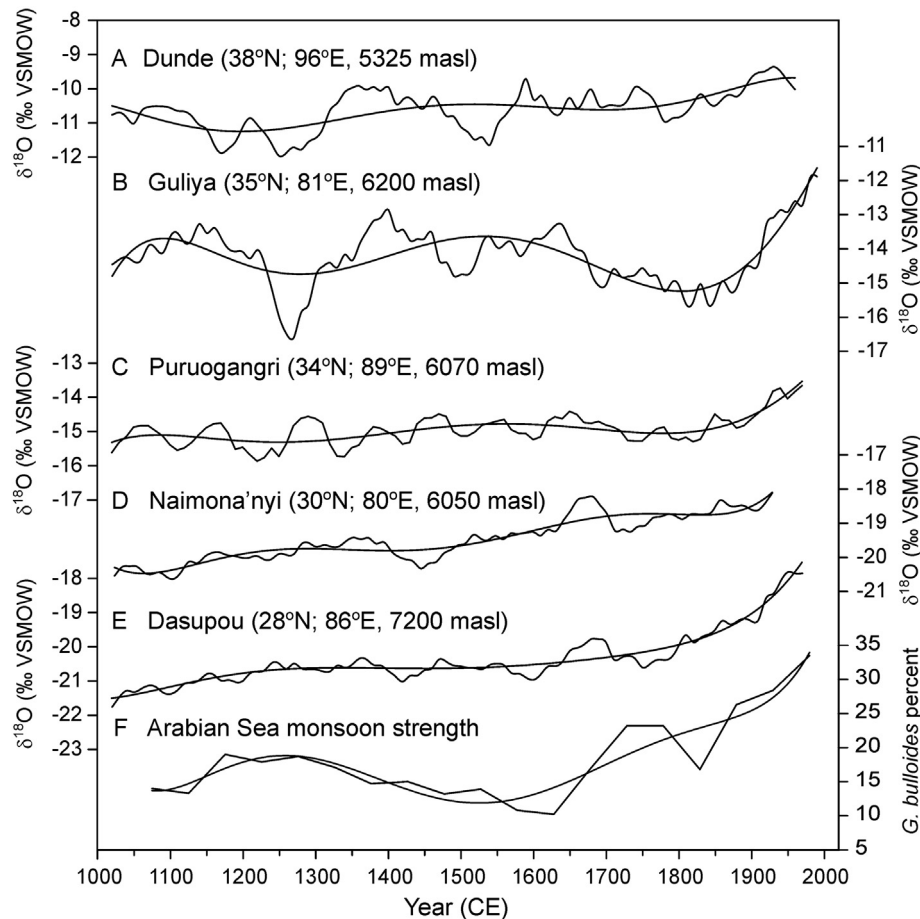


**Fig. 9.** TP ice core climate records over the last millennium.  $\delta^{18}\text{O}$  records since 1000 CE from five Third Pole ice cores (A–E) arranged from (A) Dunde at 38°N to (E) Dasuopu at 28°N. The Guliya record (B) is a composite of the 1992 plateau core from 1000 to 1840 CE and the 2015 GP time series from 1840 to 2015 CE. The Puruogangri record (C) is the average of two cores drilled on different domes. The Naimona'nyi record (D) ends at 1950 CE. All records are smoothed with 5-decade moving averages and low-frequency variations are demonstrated by 6<sup>th</sup>-order regressions. (F) Arabian Sea monsoon strength derived from a marine core *G. bulloides* record (Anderson et al., 2002).

Although the Guliya  $\delta^{18}\text{O}$  time series displays the most variability with a low-amplitude oscillation, it is consistent with the other records that all show an accelerating  $^{18}\text{O}$  enrichment (i.e., warming) from the end of the Little Ice Age to the present and with other paleoclimate proxy records, such as tree rings, that also show rapid warming in Asia since the early 19th century (PAGES 2k Consortium, 2013). For those sites that are under some degree of direct monsoon influence (Dasuopu and to a lesser extent Puruogangri) this rate of increase is unprecedented since 1000 CE. The post-1950 CE section of the Naimona'nyi record is missing, most likely the result of recent surface ablation (Kehrwald et al., 2008). Dunde, the northernmost site, shows the smallest rate of recent  $\delta^{18}\text{O}$  increase; however, this record ends in 1987 when the cores were drilled. The largest rate of  $^{18}\text{O}$  enrichment since 1800 CE

occurs on Guliya (0.2‰/decade), and the rate accelerated after ~1950 CE. This may be due to its location in the far northwest, where it receives the lowest summer precipitation and is most directly affected by North Atlantic oceanic/atmospheric processes which have undergone rapid warming in recent decades as shown by northern Greenland ice core and borehole data (Orsi et al., 2017). However, unlike the isotopic records from the southern cores, the recent Guliya  $^{18}\text{O}$  enrichment rate is not unprecedented in the last millennium since a comparable increase of 4‰ occurred from ~1250 to ~1400 CE.

The polynomial function superimposed on the Guliya  $\delta^{18}\text{O}$  record (Fig. 9B) reveals minima that occur ~550 years apart, at ~1250 and ~1800 CE. A similar periodicity has been noticed throughout the Holocene in North Atlantic marine sediment cores (Chapman

and Shackleton, 2000), which was attributed to cyclical variations in the North Atlantic Deep Water (NADW) circulation associated with solar-linked atmospheric circulation variations over Greenland (Stuvier et al., 1995). A 550-year cycle was observed in East Asian pollen records (Xu et al., 2014), also suggested to be linked to solar variations that affect high latitude climate. This multi-centennial North Atlantic influence, while most obvious in the western Kunlun ice core, is considerably muted in the Dunde record and is absent in the records from the monsoon and transition regions. Nevertheless, this periodicity in the Guliya  $\delta^{18}\text{O}$  record is preliminary, and must be validated in a time series that extends through the Holocene.

## 6. The status of Third Pole glaciers and directions for future research

### 6.1. Recent warming over the Third Pole

The northern part of Third Pole is experiencing a strong warming and since 1900 the annual average temperature for China (including the TP) has risen  $\sim 1^\circ\text{C}$  (Li et al., 2010). Between 1954 and 2006 this warming was most pronounced in winter, but in the latter part of this period (1979–2006) the greatest warming shifted to spring when temperatures increased rapidly ( $+0.5^\circ\text{C}/\text{decade}$ ) in northern China, including the northwestern region of the TP where the Kunlun Mountains are located. Elevation-dependent warming (EDW), which is pronounced in autumn and winter, is especially marked on the TP as temperatures have risen in recent decades (Liu and Chen, 2000; Pepin et al., 2015; Yan and Liu, 2014; You et al., 2008). Using a Moderate Resolution Imaging Spectroradiometer (MODIS) monthly averaged land surface temperature product, Qin et al. (2009) found that since 2000 the TP has experienced a more rapid warming than the surrounding regions. The use of MODIS is necessary as the number of weather stations administered by the China Meteorological Administration is limited in the western TP and nonexistent in areas above 4800 masl. The MODIS results indicate that the rate of warming increases from 3000 to 4800 masl, and then stabilizes or declines slightly at the highest elevations. Using a global database of 1084 high-elevation stations, Pepin and Lundquist (2008) found that 20th century temperature increases are most rapid near the annual  $0^\circ\text{C}$  isotherm due to snow-ice feedback. The data also suggest that exposed mountain summits that are located far from the effects of urbanization and topographic sheltering (such as the western Kunlun Mountains) may provide relatively unbiased records of regional to global climate.

A longer temporal perspective of EDW on the TP is illustrated by the  $\delta^{18}\text{O}$  records from the ice cores. Averages of Dunde, Puruogangri, Guliya, and Dasuopu  $\delta^{18}\text{O}$  over the last millennium illustrate the increased rate of  $^{18}\text{O}$  enrichment with elevation from 1940 to 1989 compared to that over the previous 940 years (Fig. 10). Dasuopu, the highest elevation site, shows the greatest  $^{18}\text{O}$  enrichment in the most recent 50 years compared with the earlier period. Dunde, the lowest elevation site, shows the least enrichment. This recent enrichment with elevation is consistent with the warming trends observed by Li et al. (2010). The enhanced rate of the current warming with altitude is reflected in the ice core  $\delta^{18}\text{O}$  data, which show that the past (0–1940 CE)  $^{18}\text{O}$  depletion rate was  $-0.51\text{‰}/100\text{ m}$ , while in the most recent 50-year period the depletion rate decreased to  $-0.42\text{‰}/100\text{ m}$  (Fig. 10). This has significant implications for TP water resources and environmental changes, especially as most glaciers and snow surfaces are located above 5000 masl.

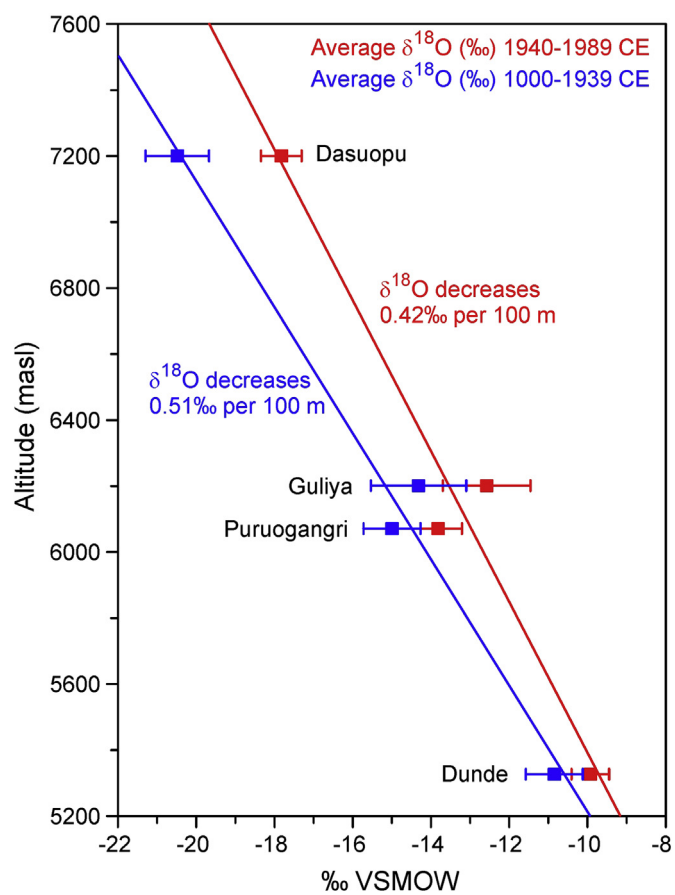


**Fig. 10.** TP ice core evidence of elevation dependent warming. The rates of change of  $\delta^{18}\text{O}$  with elevation among four TP ice core records from 1000 to 1939 CE and from 1940 to 1989 CE. The Naimona'nyi ice core does not contain ice deposited post-1950 and therefore is excluded.

### 6.2. Present and projected status of TP glaciers

Recent precipitation trends suggested by these ice core records are consistent with modern observations as shown by the Global Precipitation Climatology Project (GPCP) data (Fig. 3) in which precipitation over the Himalayas has been decreasing more than in any other region of the TP. Recent observations of  $^{18}\text{O}$  enrichment and glacier mass loss are consistent with IPCC AR5 projections (Vaughan et al., 2013) for enhanced atmospheric warming at high elevations in the low latitudes. Much of the documented ice loss on high-elevation glaciers on the western TP is more pronounced on the glacier tops than along the margins. Nuclear atmospheric tests, particularly the IVY marine tests beginning in 1952 and the Soviet atmospheric tests of 1962–63, deposited radioactive species such as  $^{36}\text{Cl}$ , tritium ( $^3\text{H}$ ),  $^{90}\text{Sr}$  and  $^{137}\text{Cs}$  on glaciers and ice sheets around the world. This top-down loss of ice on the TP was noticed in the Naimona'nyi ice core, which lacked the activity signals from both 1962/63  $^{90}\text{Sr}$  and  $^{137}\text{Cs}$  and the 1950s  $^{36}\text{Cl}$  dispersals due to vertical ablation from the surface (Kehrwald et al., 2008). More recent studies confirm that these radioactive layers have disappeared from the Lanong Glacier in southern Tibet and the Guoqu Glacier in central Tibet (Kang et al., 2015). Unfortunately, vertical ablation is difficult to detect by remote sensing, which is much more suited to measuring the areal extent of ice.

Evidence is growing that environmental conditions on the Third Pole, along with the rest of the world, have changed significantly in the last century. Marzeion et al. (2014) indicate that the

anthropogenic signal is detectable with high confidence in global glacier mass balance observations between 1991 and 2010 and place the anthropogenic contribution of mass loss during that period at  $69\% \pm 24\%$ , although no specific data exist for west central Asia. These changes and those anticipated in the future raise the prospect of significant impacts on those who depend on TP resources and its environment. The national and international importance of this region is documented by the 2012 National Academy of Sciences publication: *Himalayan Glaciers: Climate Change, Water Resources and Water Security* (National Research Council, 2012). A global temperature rise of  $1.5^\circ\text{C}$ , which is the desired limit of the 2015 Paris Climate Agreement, is projected to result in an increase of  $2.1 \pm 0.1^\circ\text{C}$  in High Asia, including the western TP (Kraaijenbrink et al., 2017). Under the RCP 2.6 to RCP 8.5 projections,  $36 \pm 7$  to  $64 \pm 5\%$  of glacier ice in this region will disappear by 2100 CE, with glaciers on the eastern and southern TP experiencing the most loss (50–75%). However, the projections are not as dire for the western Kunlun Mountains and the Karakorum, which may lose only 25% of their glacier ice by 2100 CE.

A compilation of numerous studies based on remote sensing images and topographic maps show systematic regional differences in glacier retreat since the 1970s, with the greatest decrease in length, area and mass balance occurring in the Himalayas and decreasing toward the northwest (Yao et al., 2012). The smallest reductions in length and area have occurred in the eastern Pamirs, where even positive mass balances are observed. This pattern corresponds to precipitation variations from 1979 to 2014 from the GPCP which illustrates decreasing trends in the Himalayan region and increasing trends through the western Kunlun Mountains and the Pamirs (Fig. 3), which is consistent with the recent net balance records from the Dasuopu (Thompson et al., 2000) and Guliya (Thompson et al., 2006a) ice cores. Glaciers respond to climate change over time scales that vary from years to centuries, but factors other than precipitation and temperature variations also influence their responses. For example, radiation-absorbing aerosols such as desert dust and black carbon may accelerate the warming of the atmosphere and contribute to snowpack melting and glacial retreat due to snow surface albedo changes (Painter et al., 2012). Submicron particulate pollution, which has been increasing in the northern Indian atmosphere in recent decades, may also affect orographic precipitation (Rosenfeld et al., 2007). These small particulates serve as cloud condensation nuclei around which very small drops form that are less efficient precipitation progenitors. This process may reduce precipitation in the Himalayas, even if the Indian subcontinent may not have experienced drastically decreased summer monsoon activity in recent decades (Fig. 7F).

### 6.3. Directions for future research

Ground-based evidence for recent ice loss on these few glaciers, even at elevations above 6000 masl, calls for a larger-scale assessment of vertical ice loss on glaciers across this hydrologically important region. The study of small to mid-size TP glaciers, with their profound variations in scale, topography and microclimates, provide unique challenges for both satellite and field-based observations. A number of recent papers have presented various conclusions about glacier shrinkage in the Himalaya (e.g., Bolch et al., 2012; Jacob et al., 2012; Yao et al., 2012), but all emphasize the necessity for a more comprehensive study of the region to gain a better understanding of the drivers of glacier changes in a longer-term frame of reference. Mass balance has been assessed over three consecutive years for only 15 glaciers across the TP and as yet there are no published measurements from the western Kunlun region (Yao et al., 2012).

Valuable ice archives are rapidly diminishing so new methods of

investigation are needed to extract and analyze the ice, both in the field and in the lab, with the maximum achievable resolution. Recovery and research should focus on ice cores from glaciers at risk of disappearing, using new and fast methods of glaciological investigation to retrieve the cores quickly and to understand climatic and environmental processes that might help guide mitigation and adaptation approaches to climate change. Many key areas affected by these ice archives are experiencing geopolitical as well as climatic risks. For example, the Indus River, with its source from glaciers just to the south of the western Kunlun Mountains, receives ~40% of its water discharge from glacier melt in the dry season. It flows through three countries (Pakistan, India and the western Tibet region of China) that are experiencing political tensions and in possession of nuclear weapon capabilities. Many of these geopolitical tensions arise from border disputes and cultural differences, but the competition for water is already growing and promises to worsen (Wilson et al., 2017), especially if dry season and/or drought discharge is impeded by TP glacier recession. Thus, there is a need for integration of paleoclimate data with modeling uncertainty assessments in order to help define such future scenarios. This is essential to better define the role of the Third Pole in regional environmental and societal development and in global climate change.

### Acknowledgments

This work was supported by the National Science Foundation Paleo Perspectives on Climate Change [Award 1502919]. The authors wish to thank two anonymous reviewers for their suggestions and comments which improved the quality of this paper. We thank all the field team members from The Byrd Polar and Climate Research Center and The Institute for Tibetan Plateau Research. We thank J. Box from the Geological Survey of Denmark and Greenland (GEUS) for the Greenland temperature data.

### Appendix A. Supplementary data

Supplementary data related to this article can be found at <https://doi.org/10.1016/j.quascirev.2018.03.003>.

### References

- An, W., Hou, S., Zhang, Q., Zhang, W., Wu, S., Xu, H., Pang, H., Wang, Y., Liu, Y., 2017. Enhanced recent local moisture recycling on the northwestern Tibetan Plateau deduced from ice core deuterium excess records. *J. Geophys. Res. Atmos.* 122. <https://doi.org/10.1002/2017JD027235>.
- Anderson, D.M., Overpeck, J.T., Gupta, A.K., 2002. Increase in the Asian southwest monsoon during the past four centuries. *Science* 297, 596–599. <https://doi.org/10.1126/science.1072881>.
- Archer, D.R., Fowler, H.J., 2004. Spatial and temporal variations in precipitation in the Upper Indus Basin, global teleconnections and hydrological implications. *Hydrol. Earth Syst. Sci.* 8, 47–61. <https://hal.archives-ouvertes.fr/hal-00304788>.
- Beaudon, E., Gabrielli, P., Sierra-Hernández, M.R., Wegner, A., Thompson, L.G., 2017. Central Tibetan Plateau atmospheric trace metals contamination: a 500-year record from the Puruogangri ice core. *Sci. Total Environ.* 601, 1349–1363. <https://doi.org/10.1016/j.scitotenv.2017.05.195>.
- Blanford, H.F., 1884. On the connexion of Himalayan snowfall and seasons of drought in India. *Proc. R. Acad. Lond.* 37, 3–22.
- Bolch, T., Kulkarni, A., Kääb, A., Huggel, C., Paul, F., Cogley, J.G., Frey, H., Kargel, J.S., Fujita, K., Scheel, M., Bajracharya, S., Stoffel, M., 2012. The state and fate of Himalayan glaciers. *Science* 336, 310–314. <https://doi.org/10.1126/science.1215828>.
- Box, J.E., Yang, L., Bromwich, D.H., Bai, L.-S., 2009. Greenland ice sheet surface air temperature variability: 1840–2007. *J. Clim.* 22, 4029–4049. <https://doi.org/10.1175/2009JCLI2816.1>.
- Chang, C.-P., Harr, P., Ju, J., 2001. Possible roles of Atlantic circulations on the weakening Indian Monsoon rainfall-ENSO relationship. *J. Clim.* 14, 2376–2380. [https://doi.org/10.1175/1520-0442\(2001\)014<2376:PROACO>2.0.CO;2](https://doi.org/10.1175/1520-0442(2001)014<2376:PROACO>2.0.CO;2).
- Chapman, M.R., Shackleton, N.J., 2000. Evidence of 550-year and 1000-year cyclicalities in North Atlantic circulation patterns during the Holocene. *Holocene* 10, 287–291. <https://doi.org/10.1191/095968300671253196>.
- Chen, F., Yu, Z., Yang, M.L., Ito, E., Wang, S.M., Madsen, D.B., Huang, X.Z., Zhao, Y.,

- Sato, T., Birks, H.J.B., Boomer, I., Chen, J.H., An, C.B., Wunermann, B., 2008. Holocene moisture evolution in arid central Asia and its out-of-phase relationship with Asian monsoon history. *Quat. Sci. Rev.* 27, 351–364. <https://doi.org/10.1016/j.quascirev.2007.10.017>.
- Davis, M.E., Thompson, L.G., Yao, T., Wang, N., 2005. Forcing of the Asian monsoon on the Tibetan Plateau: evidence from high-resolution ice core and tropical coral records. *J. Geophys. Res.* 110, D04101 <https://doi.org/10.1029/2004JD004933>.
- Ding, Y., Liu, S., Li, J., Shangguan, D., 2006. The retreat of glaciers in response to recent climate warming in western China. *Ann. Glaciol.* 43, 97–105. <https://doi.org/10.3189/172756406781812005>.
- Dong, W., Lin, Y.L., Wright, J.S., Ming, Y., Xie, Y.Y., Wang, B., Luo, Y., Huang, W.Y., Huang, J.B., Wang, L., Tian, L.D., Peng, Y.R., Xu, F.H., 2016. Summer rainfall over the southwestern Tibetan Plateau controlled by deep convection over the Indian subcontinent. *Nat. Commun.* 7, 10925. <https://doi.org/10.1038/ncomms10925>.
- Duan, K., Thompson, L.G., Yao, T., Davis, M.E., Mosley-Thompson, E., 2007. A 1000 year history of atmospheric sulfate concentrations in southern Asia as recorded by a Himalayan ice core. *Geophys. Res. Lett.* 34, L01810 <https://doi.org/10.1029/G1027456>.
- Dyurgerov, M., Meier, M., Armstrong, R., 2002. *Glacier Mass Balance and Regime: Data of Measurement and Analysis*. INSTAAR Occasional Paper 55.
- Fang, Y., Chang, W., Zhang, Y., Wang, N., Zhao, S., Zhou, C., Chen, X., Bao, A., 2016. Changes in inland lakes on the Tibetan Plateau over the past 40 years. *J. Geogr. Sci.* 26, 415–438. <https://doi.org/10.1007/s11442-016-1277-0>.
- Feng, S., Hu, Q., 2005. Regulation of Tibetan Plateau heating on variation of Indian summer monsoon in the last two millennia. *Geophys. Res. Lett.* 32, L02702 <https://doi.org/10.1029/2004GL021246>.
- Feng, S., Hu, Q., 2008. How the North Atlantic Multidecadal Oscillation may have influenced the Indian summer monsoon during the past two millennia. *Geophys. Res. Lett.* 35, L01707 <https://doi.org/10.1029/2007GL032484>.
- Ge, F., Sielmann, F., Zhu, X., Fraedrich, K., Zhi, X., Peng, T., Wang, L., 2017. The link between Tibetan Plateau monsoon and Indian summer precipitation: a linear diagnostic perspective. *Clim. Dynam.* <https://doi.org/10.1007/s00382-017-3585-1>.
- Gong, D.-Y., Ho, C.-H., 2002. The Siberian High and climate change over middle to high latitude Asia. *Theor. Appl. Climatol.* 72, 1–9. <https://doi.org/10.1007/s007040200008>.
- Goswami, B.N., Madhusoodanan, M.S., Neema, C.P., Sengupta, D., 2006. A physical mechanism for North Atlantic SST influence on the Indian summer monsoon. *Geophys. Res. Lett.* 33, L02706 <https://doi.org/10.1029/2005GL024803>.
- Gupta, A.K., Anderson, D.M., Overpeck, J.T., 2003. Abrupt changes in the Asian southwest monsoon during the Holocene and their links to the North Atlantic Ocean. *Nature* 421, 354–357. <https://doi.org/10.1038/nature01340>.
- Henderson, K.A., 2002. *An Ice Core Paleoclimate Study of Windy Dome, Franz Josef Land (Russia): Development of a Recent Climate History for the Barents Sea*. PhD Dissertation. The Ohio State University, p. 217.
- Huang, B., Banzon, V.F., Freeman, E., Lawrimore, J., Liu, W., Peterson, T.C., Smith, T.M., Thorne, P.W., Woodruff, S.D., Zhang, H.-M., 2015. Extended reconstructed sea surface temperature version 4 (ERSST.v4). Part I: upgrades and inter-comparisons. *J. Clim.* 28, 911–930. <https://doi.org/10.1175/JCLI-D-14-00006.1>.
- Hurrell, J.W., 1995. Decadal trends in the North Atlantic Oscillation: regional temperatures and precipitation. *Science* 269, 676–679. <https://doi.org/10.1126/science.269.5224.676>.
- Hurrell, J.W., 1996. Influence of variations in extratropical wintertime teleconnections on Northern Hemisphere. *Geophys. Res. Lett.* 23, 665–668. <https://doi.org/10.1029/96GL00459>.
- Immerzeel, W.W., van Beek, L.P.H., Bierkens, M.F.P., 2010. Climate change will affect Asian water towers. *Science* 328, 1382–1385. <https://doi.org/10.1126/science.1183188>.
- Jacob, T., Wahr, J., Pfeffer, W.T., Swenson, S., 2012. Recent contributions of glaciers and ice caps to sea level rise. *Nature* 482, 514–518. <https://doi.org/10.1038/nature10847>.
- Kang, S., Wang, F., Morgenstern, U., Zhang, Y., Grighom, B., Kaspari, S., Schwikowski, M., Ren, J., Yao, T., Qin, D., Mayewski, P.A., 2015. Dramatic loss of glacier accumulation area on the Tibetan Plateau revealed by ice core tritium and mercury records. *Cryosphere* 9, 1213–1222. <https://doi.org/10.5194/tc-9-1213-2015>.
- Kehrwald, N.M., Thompson, L.G., Yao, T.D., Mosley-Thompson, E., Schotterer, U., Alifimov, V., Beer, J., Eikenberg, J., Davis, M.E., 2008. Mass loss on Himalayan glacier endangers water resources. *Geophys. Res. Lett.* 35, L22503 <https://doi.org/10.1029/2008GL035556>.
- Kraaijenbrink, P.D.A., Bierkens, M.F.P., Lutz, A.F., Immerzeel, W.W., 2017. Impact of a global temperature rise of 1.5 degrees Celsius on Asia's glaciers. *Nature* 549, 257–260. <https://doi.org/10.1038/nature23878>.
- Lei, Y., Tian, L., Bird, B.W., Hou, J., Ding, L., Oimahmadov, I., Gadoev, M., 2014. A 2540-year record of moisture variations derived from lacustrine sediment (Sasikul Lake) on the Pamir Plateau. *Holocene* 24 (7), 761–770. <https://doi.org/10.1177/0959683614530443>.
- Li, Q., Dong, W., Li, W., Gao, X., Jones, J.P.P., Kennedy, J., Parker, D., 2010. Assessment of the uncertainties in temperature change in China during the last century. *Chin. Sci. Bull.* 55, 1974–1982. <https://doi.org/10.1007/s11434-010-3209-1>.
- Liu, W., Huang, B., Thorne, P.W., Banzon, V.F., Zhang, H.-M., Freeman, E., Lawrimore, J., Peterson, T.C., Smith, T.M., Woodruff, S.D., 2015. Extended reconstructed sea surface temperature version 4 (ERSST.v4): Part II. Parametric and structural uncertainty estimations. *J. Clim.* 28, 931–951. <https://doi.org/10.1175/JCLI-D-14-00007.1>.
- Liu, X., Chen, B., 2000. Climatic warming in the Tibetan Plateau during recent decades. *Int. J. Climatol.* 20, 1729–1742.
- Marzeion, B., Cogley, J.G., Richter, K., Parkes, D., 2014. Attribution of global glacier mass loss to anthropogenic and natural causes. *Science* 345, 919–921. <https://doi.org/10.1126/science.1254702>.
- Mohtadi, M., Prange, M., Oppo, D.W., De Pol-Holz, R., Merkel, U., Zhang, X., Steinke, S., Lückge, A., 2014. North Atlantic forcing of tropical Indian Ocean climate. *Nature* 509, 76–80. <https://doi.org/10.1038/nature13196>.
- National Research Council, 2012. *Himalayan Glaciers: Climate Change, Water Resources, and Water Security*. The National Academies Press, Washington, DC.
- Orsi, A.J., Kawamura, K., Masson-Delmotte, V., Fettweis, X., Box, J.E., Dahl-Jensen, D., Clow, G.D., Landais, A., Severinghaus, J.P., 2017. The recent warming trend in North Greenland. *Geophys. Res. Lett.* 44, 6235–6243. <https://doi.org/10.1002/2016GL072212>.
- PAGES 2k Consortium, 2013. Continental-scale temperature variability during the past two millennia. *Nat. Geosci.* 6, 339–346. <https://doi.org/10.1038/NNGEO1797>.
- Painter, T.H., Skiles, S.M., Deems, J.S., Bryant, A.C., Landry, C.C., 2012. Dust radiative forcing in snow of the Upper Colorado Basin: 1. A 6 year record of energy balance, radiation, and dust concentrations. *Water Resour. Res.* 48, W07521 <https://doi.org/10.1029/2012WR011985>.
- Pepin, N.C., Lundquist, J.D., 2008. Temperature trends at high elevations: patterns across the globe. *Geophys. Res. Lett.* 35, L14701 <https://doi.org/10.1029/2008GL034026>.
- Pepin, N., Bradley, R.S., Diaz, H.F., Baraer, M., Caceres, E.B., Forsythe, N., Fowler, H., Greenwood, G., Hashmi, M.Z., Liu, X.D., Miller, J.R., Ning, L., Ohmura, A., Palazzi, E., Rangwala, I., Schonher, V., Severskiy, I., Shahgedanova, M., Wang, M.B., Williamson, N., Yang, D.Q., 2015. Elevation-dependent warming in mountain regions of the world. *Nat. Clim. Change* 5, 424–430. <https://doi.org/10.1038/nclimate2563>.
- Qian, W., Quan, L., Shi, S., 2002. Variations of the dust storm in China and its climatic control. *J. Clim.* 15 (10), 1216–1229. [https://doi.org/10.1175/1520-0442\(2002\)015<1216:VOTDSI>2.0.CO;2](https://doi.org/10.1175/1520-0442(2002)015<1216:VOTDSI>2.0.CO;2).
- Qin, J., Yang, K., Liang, S., Guo, X., 2009. The altitudinal dependence of recent rapid warming over the Tibetan Plateau. *Clim. Change* 97, 321–327. <https://doi.org/10.1007/s10584-009-9733-9>.
- Ramisch, A., Lockot, G., Haberzettl, T., Hartmann, K., Kuhn, G., Lehmkuhl, F., Schimpf, S., Schulte, P., Stauch, G., Wang, R., Wünnemann, B., Yan, D., Zhang, Y., Diekmann, B., 2016. A persistent northern boundary of Indian summer monsoon precipitation over Central Asia during the Holocene. *Sci. Rep.* 6, 25791. <https://doi.org/10.1038/srep25791>.
- Riaz, S.M.F., Iqbal, M.J., Baig, M.J., 2017. Influence of Siberian high on temperature variability over northern areas of south Asia. *Meteorol. Atmos. Phys.* <https://doi.org/10.1007/s00703-017-0531-z>.
- Rigor, I.G., Colony, R.L., Martin, S., 2000. Variations in surface air temperature observations in the Arctic, 1979–97. *J. Clim.* 13, 896–914. [https://doi.org/10.1175/1520-0442\(2000\)013<0896:VISATO>2.0.CO;2](https://doi.org/10.1175/1520-0442(2000)013<0896:VISATO>2.0.CO;2).
- Rosenfeld, D., Dai, J., Yu, X., Yao, Z., Xu, X., Yang, X., Du, C., 2007. Inverse relations between amounts of air pollution and orographic precipitation. *Science* 315, 1396–1398.
- Roxy, M.K., Ritika, K., Terray, P., Murtugudde, R., Ashok, K., Goswami, B.N., 2015. Drying of Indian subcontinent by rapid Indian Ocean warming and a weakening land-sea thermal gradient. *Nat. Commun.* 6, 1–10. <https://doi.org/10.1038/ncomms8423>.
- Schlesinger, M.E., Ramankutty, N., 1994. An oscillation in the global climate system of period 65–70 years. *Nature* 367, 723–726. <https://doi.org/10.1038/367723a0>.
- Sierra-Hernández, M.R., Gabrielli, P., Beaudon, E., Wegner, A., Thompson, L.G., 2018. Atmospheric depositions of natural and anthropogenic trace elements on the Guliya ice cap (Northwestern Tibetan Plateau) during the last 340 years. *Atmos. Environ.* 176, 91–102.
- Stuvier, M., Grootes, P.M., Braziunas, T.F., 1995. The GISP2  $\delta^{18}\text{O}$  climate record of the past 16,500 years and the role of the Sun, ocean and volcanoes. *Quat. Res.* 44, 341–354.
- Thompson, L.G., Mosley-Thompson, E., Davis, M.E., Bolzan, J.F., Dai, J., Yao, T., Gundestrup, N., Wu, X., Klein, L., Xie, Z., 1989. Holocene-Late Pleistocene climatic ice core records from Qinghai-Tibetan Plateau. *Science* 246, 474–477. <https://doi.org/10.1126/science.246.4929.474>.
- Thompson, L.G., Mosley-Thompson, E., Davis, M.E., Bolzan, J.F., Dai, J., Klein, L., Gundestrup, N., Yao, T., Wu, X., Xie, Z., 1990. Glacial Stage ice core records from the subtropical Dunde ice cap, China. *Ann. Glaciol.* 14, 288–297.
- Thompson, L.G., Yao, T., Davis, M.E., Henderson, K.A., Mosley-Thompson, E., Lin, P.-N., Beer, J., Synal, H.-A., Cole-Dai, J., Bolzan, J.F., 1997. Tropical climate instability: the last glacial cycle from a Qinghai-Tibetan ice core. *Science* 276, 1821–1825. <https://doi.org/10.1126/science.276.5320.1821>.
- Thompson, L.G., Yao, T., Mosley-Thompson, E., Davis, M.E., Henderson, K.A., Lin, P.-N., 2000. A high-resolution millennial record of the South Asian Monsoon from Himalayan ice cores. *Science* 289, 1916–1919. <https://doi.org/10.1126/science.289.5486.1916>.
- Thompson, L.G., Davis, M.E., Mosley-Thompson, E., Lin, P.-N., Henderson, K.A., Mashiotta, T.A., 2005. Tropical ice core records: evidence for asynchronous glaciation on Milankovitch timescales. *J. Quat. Sci.* 20, 723–733. <https://doi.org/10.1002/jqs.972>.
- Thompson, L.G., Mosley-Thompson, E., Brecher, H., Davis, M.E., Leon, B., Les, D., Mashiotta, T.A., Lin, P.-N., Mountain, K., 2006a. Evidence of abrupt tropical

- climate change: past and present. *PNAS* 103 (28), 10536–10543. <https://doi.org/10.1073/pnas.0603900103>.
- Thompson, L.G., Yao, T., Davis, M.E., Mosley-Thompson, E., Mashiotta, T.A., Lin, P.-N., Mikhalenko, V.N., Zagorodnov, S., 2006b. Holocene climate variability archived in the Puruogangri ice cap from the central Tibetan Plateau. *Ann. Glaciol.* 43, 61–69.
- Thompson, L.G., Mosley-Thompson, E., Davis, M.E., Brecher, H.H., 2011. Tropical glaciers, recorders and indicators of climate change, are disappearing globally. *Ann. Glaciol.* 52, 23–34.
- Tian, L., Masson-Delmotte, V., Stievenard, M., Yao, T., Jouzel, J., 2001. Tibetan Plateau summer monsoon northward extent revealed by measurements of water stable isotopes. *J. Geophys. Res.* 106 (D22), 28,081–28,088. <https://doi.org/10.1029/2001JD900186>.
- Tian, L., Yao, T., Schuster, P.F., White, J.W.C., Ichiyangi, K., Pendall, E., Pu, J., Yu, W., 2003. Oxygen-18 concentrations and ice cores on the Tibetan Plateau. *J. Geophys. Res.* 108, 4293. <https://doi.org/10.1029/2002JD002173>.
- Tian, L., Yao, T., Li, Z., MacClune, K., Wu, G., Xu, B., Li, Y., Lu, A., Shen, Y., 2006. Recent rapid warming trend revealed from the isotopic record in Muztagata ice core, eastern Pamirs. *J. Geophys. Res.* 111, D13103. <https://doi.org/10.1029/2005JD006249>.
- Tian, L., Yao, T., MacClune, K., White, J.W.C., Schilla, A., Vaughn, B., Vachon, R., Ichiyangi, K., 2007. Stable isotopic variations in west China: a consideration of moisture sources. *J. Geophys. Res.* 112, D10112. <https://doi.org/10.1029/2006JD007718>.
- Trenberth, K.E., Hurrell, J.W., 1994. Decadal ocean–atmosphere variations in the Pacific. *Clim. Dynam.* 9, 303–309.
- Treydte, K.S., Schleser, G.H., Helle, G., Frank, D.C., Winiger, M., Haug, G.H., Esper, J., 2006. The twentieth century was the wettest period in northern Pakistan over the past millennium. *Nature* 440, 1179–1182. <https://doi.org/10.1038/nature04743>.
- Vaughan, D.G., Comiso, J.C., Allison, I., Carrasco, J., Kaser, G., Kwok, R., Mote, P., Murray, T., Paul, F., Ren, J., Rignot, E., Solomina, O., Steffen, K., Zhang, T., 2013. Observations: cryosphere. In: Stocker, T.F., Qin, D., Plattner, G.-K., Tignor, M., Allen, S.K., Boschung, J., Nauels, A., Xia, Y., Bex, V., Midgley, P.M. (Eds.), *Climate Change 2013: the Physical Science Basis. Contribution of Working Group I to the Fifth Assessment Report of the Intergovernmental Panel on Climate Change*. Cambridge University Press, Cambridge, United Kingdom and New York, NY, USA.
- Walker, G.T., 1910. On the meteorological evidence for supposed changes of climate in India. *Mem. Indian Meteorol.* 21, 1–21.
- Wang, S., Gong, D., 2000. Enhancement of the warming trend in China. *Geophys. Res. Lett.* 27, 2581–2584. <https://doi.org/10.1029/1999GL010825>.
- Wang, B., Liu, J., Kim, H.-J., Webster, P.J., Yim, S.-Y., Xiang, B., 2013. Northern Hemisphere summer monsoon intensified by mega-El Niño/southern oscillation and Atlantic multidecadal oscillation. *PNAS* 110, 5347–5352. <https://doi.org/10.1073/pnas.1219405110>.
- Wang, N., Thompson, L.G., Davis, M.E., Mosley-Thompson, E., Yao, T., Pu, J., 2003. Influence of variations in NAO and SO on air temperature over the northern Tibetan Plateau as recorded by  $\delta^{18}\text{O}$  in the Malan ice core. *Geophys. Res. Lett.* 30 (22), 2167. <https://doi.org/10.1029/2003GL018188>.
- Wang, H., Wang, W., Yin, C., Wang, Y., Lu, W., 2006. Littoral zones as the “hotspots” of nitrous oxide ( $\text{N}_2\text{O}$ ) emission in a hyper-eutrophic lake in China. *Atmos. Environ.* 40, 5522–5527. <https://doi.org/10.1016/j.atmosenv.2006.05.032>.
- Wang, J., Yang, B., Qin, C., Kang, S., He, M., Wang, Z., 2014. Tree-ring inferred annual mean temperature variations on the southeastern Tibetan Plateau during the last millennium and their relationships with the Atlantic multidecadal oscillation. *Clim. Dynam.* 43, 627–640. <https://doi.org/10.1007/s00382-013-1802-0>.
- Wilson, A.M., Gladfelter, S., Williams, M.W., Shahi, S., Baral, P., Armstrong, R., Racoviteanu, A., 2017. High Asia: the international dynamics of climate change and water security. *J. Asian Stud.* 76, 457–480. <https://doi.org/10.1017/S0021911817000092>.
- Wu, B., 2005. Weakening of Indian summer monsoon in recent decades. *Adv. Atmos. Sci.* 22, 21–29.
- Wu, T.-W., Qian, Z.-A., 2003. The relation between the Tibetan winter snow and the Asian summer monsoon and rainfall: an observational investigation. *J. Clim.* 16, 2038–2051. [https://doi.org/10.1175/1520-0442\(2003\)016<2038:TRBTTW>2.0.CO;2](https://doi.org/10.1175/1520-0442(2003)016<2038:TRBTTW>2.0.CO;2).
- Xin, X., Zhou, T., Yu, R., 2010. Increased Tibetan Plateau snow depths: an indicator of the connection between enhanced winter NAO and late-Spring tropospheric cooling over East Asia. *Adv. Atmos. Sci.* 27 (4), 788–794. <https://doi.org/10.1007/s00376-009-9071-x>.
- Xu, D., Lu, H., Chu, G., Wu, N., Shen, C., Wang, C., Mao, L., 2014. 500-year climate cycles stacking of recent centennial warming documented in an East Asian pollen record. *Sci. Rep.* 4, 3611. <https://doi.org/10.1038/srep03611>.
- Yan, L., Liu, X., 2014. Has climatic warming over the Tibetan Plateau paused or continued in recent years? *J. Earth Ocean Atmos. Sci.* 1, 13–28.
- Yang, M., Yao, T.-D., He, Y., Thompson, L.G., 2000. ENSO events recorded in the Guliya ice core. *Clim. Change* 47, 401–409.
- Yao, T., Thompson, L.G., Mosley-Thompson, E., Zhihong, Y., Xingping, Z., Lin, P.-N., 1996. Climatological significance of  $\delta^{18}\text{O}$  in north Tibetan ice cores. *J. Geophys. Res.* 101 (D23), 29,531–29,537.
- Yao, T., Shi, Y., Thompson, L.G., 1997. High resolution record of paleoclimate since the Little Ice Age from the Tibetan ice cores. *Quat. Int.* 37, 19–23. [https://doi.org/10.1016/1040-6182\(96\)00006-7](https://doi.org/10.1016/1040-6182(96)00006-7).
- Yao, T., Xiang, S., Zhang, X., Wang, N., Wang, Y., 2006. Microorganisms in the Malan ice core and their relation to climatic and environmental changes. *Global Biogeochem. Cycles* 20, GB1004. <https://doi.org/10.1029/2004GB002424>.
- Yao, T., Thompson, L., Yang, W., Yu, W.S., Gao, Y., Guo, X.J., Yang, X.X., Duan, K.Q., Zhao, H.B., Xu, B.Q., Pu, J.C., Lu, A.X., Xiang, Y., Kattel, D.B., Joswiak, D., 2012. Different glacier status with atmospheric circulations in Tibetan Plateau and surroundings. *Nat. Clim. Change* 2, 663–667. <https://doi.org/10.1038/NCLIMATE1580>.
- Yao, T., Masson-Delmotte, V., Gao, J., Yu, W.S., Yang, X.X., Risi, C., Sturm, C., Werner, M., Zhao, H.B., He, Y., Ren, W., Tian, L.D., Shi, C.M., Hou, S.G., 2013. A review of climatic controls on  $\delta^{18}\text{O}$  in precipitation over the Tibetan Plateau: observations and simulations. *Rev. Geophys.* 51, 525–548. <https://doi.org/10.1002/rog.20023>.
- You, Q., Kang, S., Pepin, N., Yan, Y., 2008. Relationship between trends in temperature extremes and elevation in the eastern and central Tibetan Plateau, 1961–2005. *Geophys. Res. Lett.* 35, L04704. <https://doi.org/10.1029/2007GL032669>.
- Zhang, X., Xu, B., Günther, F., Witt, R., Wang, M., Xie, Y., Zhao, H., Li, J., Gleixner, G., 2017. Rapid northward shift of the Indian monsoon on the Tibetan Plateau at the end of the Little Ice age. *J. Geophys. Res. Atmos.* 122, 9269–9279. <https://doi.org/10.1002/2017JD026849>.
- Zhang, Y., Li, T., Wang, B., 2004. Decadal change of the Spring snow depth over the Tibetan Plateau: the associated circulation and influence on the East Asian summer monsoon. *J. Clim.* 17, 2780–2793.
- Zhao, H., Moore, G.W.K., 2004. On the relationship between Tibetan snow cover, the Tibetan Plateau monsoon and the Indian summer monsoon. *Geophys. Res. Lett.* 31, L14204. <https://doi.org/10.1029/2004GL020040>.
- Zhao, H., Xu, B., Yao, T., Tian, L., Li, Z., 2011. Records of sulfate and nitrate in an ice core from Mount Muztagata, central Asia. *J. Geophys. Res.* 116, D13304. <https://doi.org/10.1029/2011JD015735>.